TIME-DOMAIN UNCOUPLED ANALYSES FOR SEISMIC ASSESSMENT OF LAND-BASED WIND TURBINES

Fabio Santangelo, Giuseppe Failla, Adolfo Santini, Felice Arena

Dipartimento di Ingegneria Civile, dell'Ambiente, dell'Energia e dei Materiali (DICEAM)

Università di Reggio Calabria, 89124 Reggio Calabria, Italy

Tel.: +39-0965-1692221. Email: giuseppe.failla@unirc.it

ABSTRACT

Seismic analysis plays an important role in the design of land-based and offshore wind turbines in areas at seismic hazard. For seismic assessment, International Standards and Guidelines allow combining two separate analyses, one under wind and another under earthquake only, as alternative to computationally expensive, fully-coupled time-domain simulations. In these uncoupled analyses, the separate earthquake response is generally computed using the standard acceleration response spectrum, upon including an additional damping referred to as *aerodynamic* damping. By a response-spectrum approach, however, important sources of nonlinearity, such as those related to foundation flexibility, cannot be properly accounted for.

Focusing on land-based wind turbines, this paper investigates a time-domain implementation of uncoupled analyses, which may involve a nonlinear foundation model. The case study is a 5 MW baseline wind turbine, resting on a pile foundation modeled by nonlinear springs. For different earthquake records and wind velocities, comparisons with fully-coupled simulations show that the combination of uncoupled analyses implemented in the time domain yields accurate results, provided that an appropriate level of aerodynamic damping is included in the model. Notably, it is seen that such aerodynamic damping level agrees with the one generally recommended for response-spectrum based uncoupled analyses.

KEYWORDS

Land-based wind turbine, Seismic response, Fully-coupled analysis, Uncoupled analyses, Aerodynamic damping

1. INTRODUCTION

In view of the increasing number of wind farms being installed in many countries of Europe, Asia and America, including seismically-active areas [1-2], the seismic assessment of land-based horizontal-axis wind turbines (HAWTs) has been the subject of several studies in the last decade. Investigations have been carried out adopting different system models, load combinations and methods of analysis [3,4]. Simplified models or full models including support structure, rotor, as well as mechanical/electrical/control components of the turbine, have been used as system models. Combinations of earthquake loads with operational wind loads or emergency-stop loads, and earthquake loads acting in parked rotor conditions with or without wind loads, have been considered as typical loading conditions. Methods of analysis have been implemented in the time domain or using the classical response spectrum approach.

Simplified finite element (FE) models have been implemented in ref. [5-7], under earthquake loads acting in parked rotor conditions without wind loads. Bazeos et al. [5] studied a 38 m high, 450 kW HAWT resting on a concrete square footing in a semi-rock soil, using shell or beam elements for the tower, a top lumped mass and a rigid block to model rotor-nacelle assembly (RNA) and square footing, respectively, springs/dashpots and added soil mass to account for soil-structure interaction [8]. Lavassas et al. [6] studied a 44 m high, 1 MW HAWT on a concrete circular footing in a rock soil, using shell elements for the tower, 3D-solid elements for the circular footing, and a top lumped mass to model the RNA. Stamatopolous [7] investigated a 53.95 m high HAWT resting on a circular footing, using beam elements for tower and blades, 3D-solid elements for the footing, nonlinear unilateral springs below the footing to model foundation flexibility. For the relatively low ground accelerations of the project sites under consideration, time-domain analyses in ref. [5] and response-spectrum based analyses in ref. [5,6] found that earthquake loads acting in parked rotor conditions, without wind loads, induce low stress levels as compared to other design loads. On the

other hand, time-domain analyses and response-spectrum based analyses in ref. [7] demonstrated that shear and bending-moment demand at the tower base can be underestimated significantly by the Greek Design Code, when near fault ground motions are considered. Notice that, in ref. [7], the response-spectrum approach was implemented on a linearized model of the structure, where the nonlinear unilateral springs below the footing are replaced with an equivalent linearly-elastic rotational spring, whose stiffness is calibrated by an approximate iterative procedure. FE models under earthquake loads and operational wind loads have been investigated in ref. [9-11]. Sapountzakis et al. [9] have proposed a FE approach formulated by the boundary element method. They studied the National Renewable Energy Laboratory (NREL) 5 MW baseline HAWT [12,13] on either surface or monopile foundation, using beam elements for the tower, a top mass for the RNA, nonlinear springs/dashpots to model foundation flexibility, and including axial load effects. Responses for surface and monopile foundations were compared under earthquake loads and a top force modeling wind loads, with the latter built by applying the combined blade element and momentum (BEM) theory on the rotor, taken as fixed on a rigid tower. A FE model accounting for flexibility of the blades in the flapping direction, bending and twisting flexibility of the tower, gyroscopic effects of the rotor, has been proposed by Diaz and Suarez [10]. They investigated the seismic response of a 76 m high, 1.65 MW HAWT, modeling the tower by beam elements and the blades by rigid rods with rotational springs at the roots. Considering four strong ground motions with operational wind loads, they showed that stresses at some tower sections may exceed those from extreme winds. A FE model of the NREL 5 MW HAWT, involving shell elements with nonlinear material behavior for the tower, beam elements for the blades and a coupling joint between rotor and rigid nacelle has been developed by Asareh [11] for fragility analyses under operational loads generated by Aerodyn [14].

In order to study the earthquake response under operational wind loads, full models including support structure and RNA components with different levels of detail, have generally been preferred over simplified models. Full system models have been used in conjunction with fully-coupled, nonlinear time-domain simulations capable of accounting for the inherent coupling between aerodynamic and seismic responses [15]. Indeed, tower top oscillations due to ground motion affect

rotor aerodynamics, in particular the relative wind speed at the blades, depending on which the aerodynamic loads, i.e. lift and drag forces on the blades, are calculated.

Fully-coupled, nonlinear time-domain simulations on full system models have been implemented in ref. [16-20]. Using FAST [21], a NREL simulation tool where motion equations of the system are derived by a combined multi-body dynamics and modal approach (for the seismic module, see in particular ref.[22,23]), Prowell et al. [16-18] showed that earthquakes may produce, in the NREL 5MW baseline HAWT, a bending-moment demand at the tower base well above the one from extreme wind events, in operational, emergency shutdown and parked simulations. Also, Prowell et al. [18] demonstrated that not only first but also second modes contribute significantly, in both fore-aft (FA) and side-to-side (SS) directions (i.e., parallel and perpendicular directions to the rotation axis of the rotor, respectively), in agreement with previous findings on the importance of the second modes in seismic response of large turbines [10,24]. Zhao et al. [19,20] developed a hybrid multi-body system (MBS) where nacelle and tower are discretized into an ensemble of rigid bodies coupled elastically by constraint joints and springs, the wind rotor is treated as a rigid disk, and a 3D set of uncoupled frequency-independent spring-damper devices, including translations and rotations, is used to model the foundation. Governing equations are derived using Lagrange's equations and no external calculation of component mode shapes is required. By the MBS approach, Zhao et al. [19] studied the seismic response of a 65 m high, 1.5 MW HAWT, showing that shear force and bending moment at the tower base are affected considerably by earthquake loads, in both FA and SS directions. This result was found for operational conditions, with a weak real earthquake record. Studies in ref. [16-20] demonstrated that earthquake loads may be design driving in regions of high seismic hazard.

Although fully-coupled, nonlinear time-domain simulations are certainly most indicated to build a numerical solution for seismic assessment, the main disadvantage is that computational costs may be significant, almost prohibitive when several analyses have to be implemented for different environmental states and system parameters, as in the early stages of design. For these reasons, a considerable attention has been devoted to assess whether the response to simultaneous wind and earthquake loads can be obtained by combining two uncoupled analyses, one under wind and

another under earthquake only, instead of running a fully-coupled analysis. In this manner, the response to a given wind state, once computed, could be combined with the response to different potential earthquake events, with a significant reduction of computational costs with respect to fully-coupled time-domain simulations.

The implementation of uncoupled analyses is currently the subject of active research. Early investigations have been made by Witcher [25]. Using GH BLADED [26], a simulation tool where equations of motion are derived by a combined multi-body dynamics and modal approach, he studied a 2MW HAWT mounted on a 60 m high steel tower, showing that, if the separate earthquake moment demand at the tower base is computed from a 5% damped FA-response spectrum and then linearly combined with the separate wind moment demand computed by a time-domain simulation, a good matching is attained with the moment demand at the tower base computed from a fully-coupled, nonlinear time-domain simulation. Considering that steel structures can reasonably be given a 1% structural damping, using a 5% damped FA-response spectrum means that an additional 4% damping is included in the FA modes, when computing the separate earthquake response. The 4% additional damping has been named as *aerodynamic* damping, to point out that its source is essentially the aerodynamics of the spinning rotor. In a rather intuitive way, aerodynamic damping arises from the observation that forward/backward motion of a structure vibrating in a wind field induces a change in the aerodynamic forces that, in general, reduce the dynamic response of the structure [27]. Following the work of Witcher [25], Asareh and Volz [28] considered a total 5% structural damping to analyze the FE model of the NREL 5 MW HAWT in ref. [11] under earthquake ground motion and operational loads generated by Aerodyn [14]. Experimental tests run on a 65 kW HAWT by Prowell et al. [16], in operational state with earthquake shaking in FA and SS directions, confirmed that aerodynamic damping effects affect the FA response, and showed that are negligible in the SS direction. Recently, an analytical estimate of aerodynamic damping has been proposed by Valamanesh and Myers [27], based on BEM theory, under the assumption of laminar flow (no turbulence) and rigid rotor. The proposed estimate was found to depend on the wind velocity. Working on a FE model of the HAWT with beam elements along the tower and lumped masses at the element nodes and top, subjected to seven ground

motions and a top thrust force built in steady-state laminar flow by FAST [21], the authors found a good agreement between top median drifts computed by combining separate wind and earthquake responses, when the earthquake response is built with either the proposed analytical estimate of aerodynamic damping depending on the wind velocity or, alternatively, with a 4% aerodynamic damping in the FA direction and 0% in the SS direction [27].

International Standards such as IEC 61400-1 [29] and Guidelines as ASCE-AWEA RP2011 [30] allow combining uncoupled analyses, instead of performing fully-coupled, nonlinear time-domain simulations. In Annex C, IEC 61400-1 [29] proposes a method to compute the response under earthquake and operational wind loads. It is based on the assumption that the whole structure is subjected to the same acceleration, computed from the first tower bending natural frequency using a 1% damped response spectrum. Stress resultants at the tower base are calculated by applying, at the tower top, a force equal to the total mass of the RNA + ½ the mass of the tower, times the design acceleration response. The corresponding base stress resultants are linearly combined with the separate wind demand, computed, in particular, from an emergency stop simulation at rated wind speed. Some prescriptions to compute the response under earthquake and operational loads are given also by ASCE-AWEA RP2011 [30]. It recommends that the separate earthquake demand is computed considering an acceleration response spectrum with 5% total damping, and combined with the operational wind demand using a combination load factor equal to 0.75. The 5% damped spectrum of ASCE-AWEA RP2011 [30] corresponds to consider 1% structural damping of steel structures + 4% aerodynamic damping, in agreement with findings of Witcher [25], Valamanesh and Myers [27].

Some insights into the uncoupled analyses prescribed by IEC 61400-1 [29] and ASCE-AWEA RP2011 [30] have been provided in ref. [17,31]. Considering the NREL 5MW baseline HAWT under a large database of earthquake records, Prowell [17] showed that the IEC method, if separate earthquake and wind demands are combined by a square root of the sum of the squares (SRSS) of the maxima instead of being linearly combined, can provide moment demands at the tower base that better match those obtained by fully-coupled, nonlinear time-domain simulations. He also showed that such SRSS combination of uncoupled analyses may predict either larger or smaller demands

than those from fully-coupled simulations (see Figure 8.11 in ref. [17]). Again for the NREL 5MW baseline HAWT, Asareh and Prowell [31] proposed a combination of uncoupled analyses where a 0.75 combination factor, as in ASCE-AWEA RP2011, is used to combine the separate operational wind and earthquake demands, with the latter computed using a 4% aerodynamic damping in the time domain or by a response-spectrum approach. The authors showed that, in this manner, the mean bending-moment demands along the tower, computed by averaging over a set of earthquake records [31], agree well with the mean demands from fully-coupled, nonlinear time-domain simulations. As in ref. [17], mean demands from the combination of uncoupled analyses were either larger or smaller than those from fully-coupled simulations. Notice that fixed foundation models were assumed in both ref. [17] and ref. [31].

It has been noted above that the uncoupled analyses allowed by IEC 61400-1 [29] and ASCE-AWEA RP2011 [30], the separate earthquake response is generally computed based on the acceleration response spectrum. When computing the earthquake response by a spectrum analysis, however, nonlinear foundation behaviour cannot be considered appropriately in the structural model, because periods T to be used in the response spectrum must be, indeed, periods of the structure assumed to behave linearly. To address these issues, uncoupled analyses where separate wind and earthquake responses are both computed in the time domain would be highly desirable, as they would allow nonlinearities, such as those deriving from foundation modelling, to be considered directly in the structural model. It is apparent, however, that the implementation of such uncoupled analyses requires an appropriate level of aerodynamic damping, on which, to the best of authors' knowledge, no data are available in the literature.

The purpose of this paper is to investigate how uncoupled analyses, including a nonlinear foundation model, can be implemented in the time domain, for the seismic assessment of land-based HAWTs. The case study is the NREL 5MW baseline wind turbine [12,13], mounted on a 87.6 m column resting on a pile-supported footing in sandy soil. For earthquake striking in operational state, fully-coupled and uncoupled analyses are implemented in the time domain using GH BLADED [26], on a full model of the system which includes support structure, rotor blades, mechanical/electrical/control components of the turbine, and nonlinear soil springs for foundation

flexibility. Considering different wind velocities and ground motions, the response from fully-coupled simulation is compared with the linear combination of separate wind and earthquake responses, the latter computed by adding different levels of aerodynamic damping in the first two FA support structure modes. The first step will be to assess whether there exists an aerodynamic damping level capable of minimizing a total error, which involves shear-force and bending-moment demands at the tower base, as computed by fully-coupled simulation and combination of uncoupled analyses. It will be found that such aerodynamic damping level cannot be obtained, for all the considered wind velocities and ground motions. However, it will be shown that errors in bending-moment and shear-force demands are within engineering margins, analogous to those encountered in the combination of response-spectrum based uncoupled analyses, if a 4% aerodynamic damping is assumed for all the considered wind velocities and ground motions. The results confirm that the 4% aerodynamic damping level, recommended by ASCE-AWEA RP2011 [30] and used in previous studies [25,27,31], can reasonably be used also in time-domain uncoupled analyses, including the considered nonlinear-spring foundation model.

The paper is organized in four Sections. The system model is presented in Section 2. Time-domain fully-coupled and uncoupled analyses will be described in Section 3. Numerical results will be discussed in Section 4. An Appendix is included.

2. SYSTEM MODEL

The turbine is the NREL 5MW baseline three-bladed turbine [12]. The support structure is a 87.6 m steel column mounted on a concrete square footing, which rests on concrete piles in a sandy soil. See Figs. 1-2 and Table 1 for wind turbine geometry and parameters, material and soil properties. The full system is implemented in GH BLADED [26]. Rotor blades, nacelle, drive train, mechanical/electrical/control components are modelled based on parameters in ref. [12], for a full representation of wind turbine aerodynamics. Shear-deformable 3D beam elements are used for blades, column and piles, while the footing is modeled as a rigid block.

Wind turbine		Material and soil properties	
Type	Horizontal axis wind turbine	**Steel (tower)**	
Power rating	5-MW	Young's modulus	210 GPa
Rotor Configuration	3 blade upwind	Poisson's ratio	0.3
Control	Variable speed, collective pitch	Mass density	7850 kg/m^3
Drivetrain	High speed, multiple-stage gearbox		
Hub Height	90 m	**Concrete (square footing and piles)**	
Cut-in Wind Speed	3 m/s	Young's modulus	31 GPa
Rated Wind Speed	11.4 m/s	Poisson's ratio	0.2
Cut-out Wind Speed	25 m/s	Mass density	2400 kg/m^3
Rotor Speed Range	6.9 to 12.1 rpm		
Rated Tip Speed	80 m/s	**Sand**	
Rotor diameter	126 m	Angle of internal friction	33°
Tower height	87.6 m	Initial modulus of subgrade reaction	16287 kN/m^3
Hub height	90 m	Effective soil weight	10 kN/m^3
Mass of rotor	111,000 kg		
Mass of nacelle	240,000 kg		
Mass of tower	347,460 kg		

Table 1. Wind turbine parameters, material and soil properties.

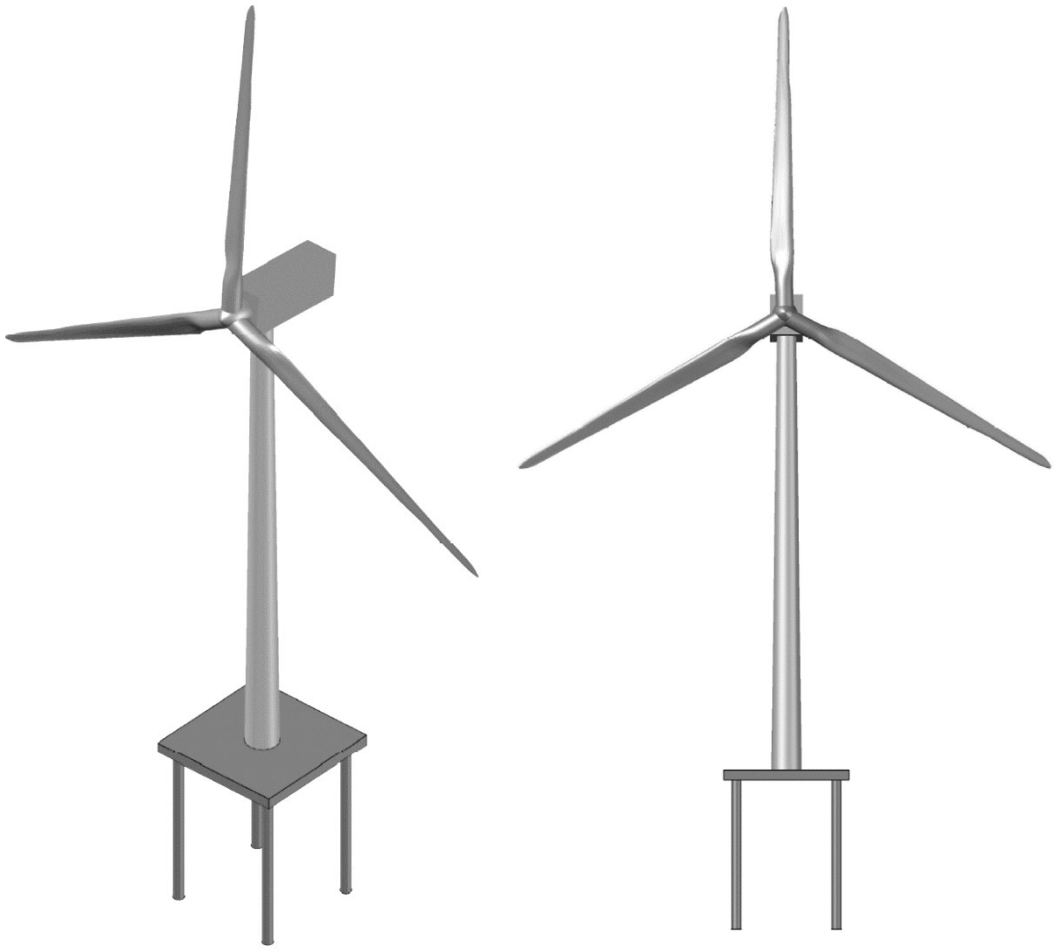

Fig. 1. 5 MW three-bladed HAWT with a steel column, resting on a concrete pile-supported square footing.

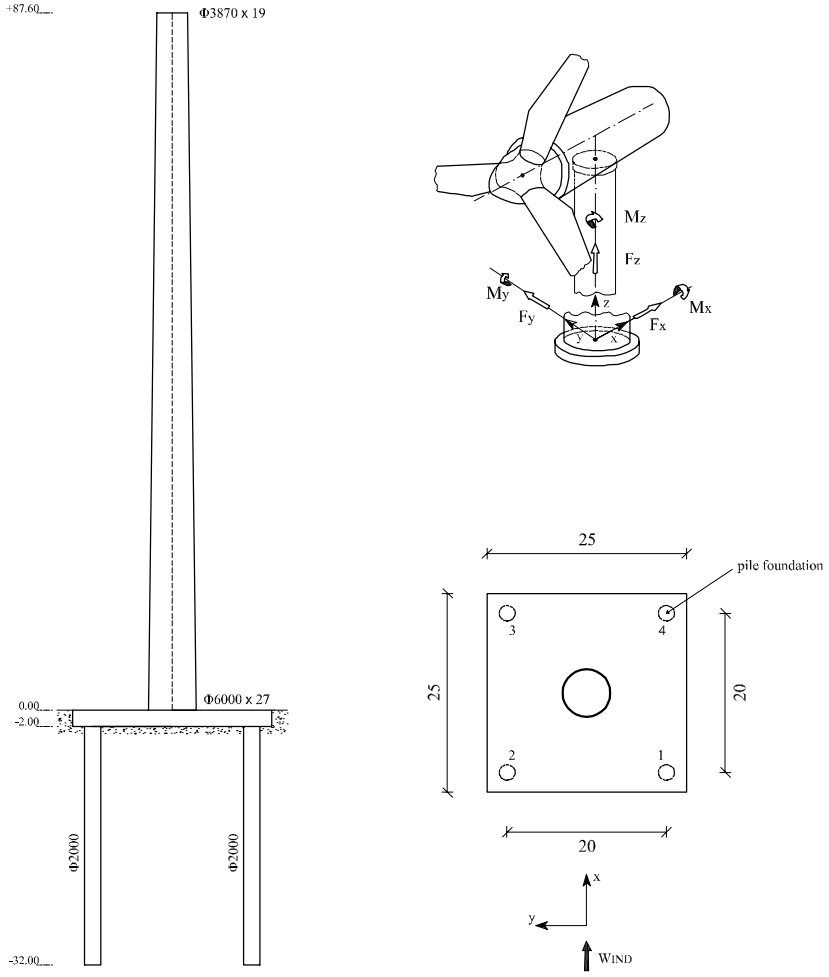

Fig. 2. Geometry and sign conventions for stress resultants at the tower base (length in m, diameter and thickness in mm).

Two different foundation models are considered:

(a) fixed (clamped base)

(b) flexible.

The flexible model involves uncoupled lateral and vertical springs along the piles at a 1 m spacing, and a vertical spring at the pile tip, as shown in Fig. 3. The springs feature nonlinear force-deflection laws given by *p-y*, *t-z* and *Q-z* curves provided by API code [32] for sandy soils (A=0.9 in Eq. (6.8.7-1) of ref. [32]). Notice that analogous models of foundation flexibility have been proposed for dynamic response of pile-supported offshore wind turbines [33-37]. Soil damping, whose role may be important under seismic excitations [38,39], is accounted for by appropriately selecting the structural damping ratios of the support structure modes, as detailed in Section 2.1. This model of soil damping effects has been already adopted in previous studies on pile-supported offshore wind turbines under dynamic loads, see ref. [40,41]. More sophisticated modelling of soil

damping, such as those involving nonlinear springs/dashpots in series and parallel, possibly including gap effects, or frequency-dependent springs/dashpots [42-46], are not allowed in GH-BLADED [26], as in similar codes for wind turbine modelling [21]. They could be implemented in standard FE codes where, however, rather simplified models of the RNA are generally used (lumped mass or fixed rotor even in operating conditions), at the expense of an accurate description of wind turbine aerodynamics. The latter is essential for the purposes of this study and can accurately be represented in GH-BLADED [26], as briefly discussed in Section 2.2.

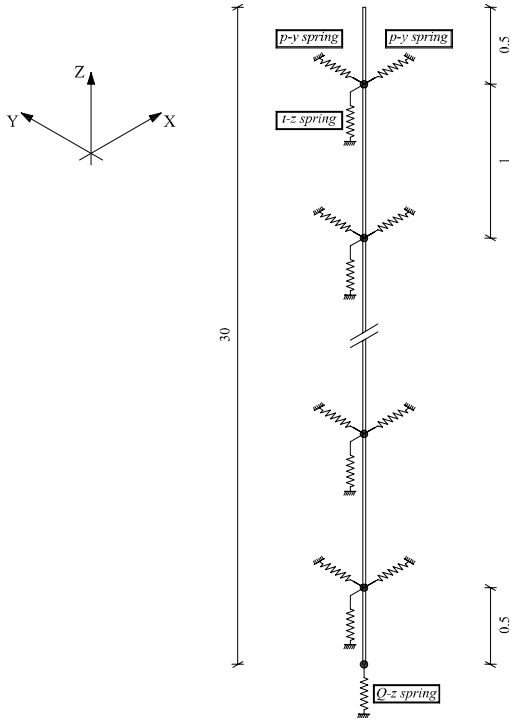

Fig. 3. Lateral and vertical springs along piles (length in m).

2.1. Modal analysis

For a first insight, modal analysis is implemented in GH BLADED [26] considering the rotor in a parked state (no rotational speed) at 0° azimuth angle (one blade upward, two blades downward). Table 2 reports the frequencies of support structure modes and blades modes, for fixed and flexible foundation models, the latter with force-deflection laws of the soil springs linearized to the initial tangent stiffness. FA and SS directions correspond to X and Y directions in Fig. 2, respectively.

For fixed foundation, the frequencies of the first and second FA and SS support structure modes, as well as the frequencies of the blade modes, are in agreement with those in the literature [13];

"yaw" and "pitch" means that the blade modes are coupled with yaw and pitch motion of the rotor [13,34]). Shapes of first and second FA support structure modes for fixed foundation are reported in Fig. 4a; those in SS direction are similar and are not reported for brevity.

As for flexible foundation, the frequencies of the first FA and SS support structure modes, and frequencies of the blade modes, are almost identical to the corresponding ones for fixed foundation, while the frequencies of second FA and SS support structure modes are decreased, in agreement with previous studies [19]. Shapes of first and second FA support structure modes for flexible foundation are shown in Fig. 4b.

Mode description	Fixed foundation Freq. (Hz)	Flexible foundation Freq. (Hz)
1st Support Structure Side-to-Side	0.316	0.313
1st Support Structure Fore-Aft	0.319	0.315
1st Blade Asymmetric Flapwise Yaw	0.645	0.644
1st Blade Asymmetric Flapwise Pitch	0.677	0.676
1st Blade Collective Flap	0.710	0.710
1st Blade Asymmetric Edgewise Pitch	1.079	1.079
1st Blade Asymmetric Edgewise Yaw	1.093	1.093
2nd Blade Asymmetric Flapwise Yaw	1.739	1.734
2nd Blade Asymmetric Flapwise Pitch	1.888	1.880
2nd Blade Collective Flap	1.998	1.997
2nd Support Structure Fore-Aft	2.836	2.349
2nd Support Structure Side-to-Side	2.995	2.359

Table 2. Natural frequencies for fixed and flexible foundation models.

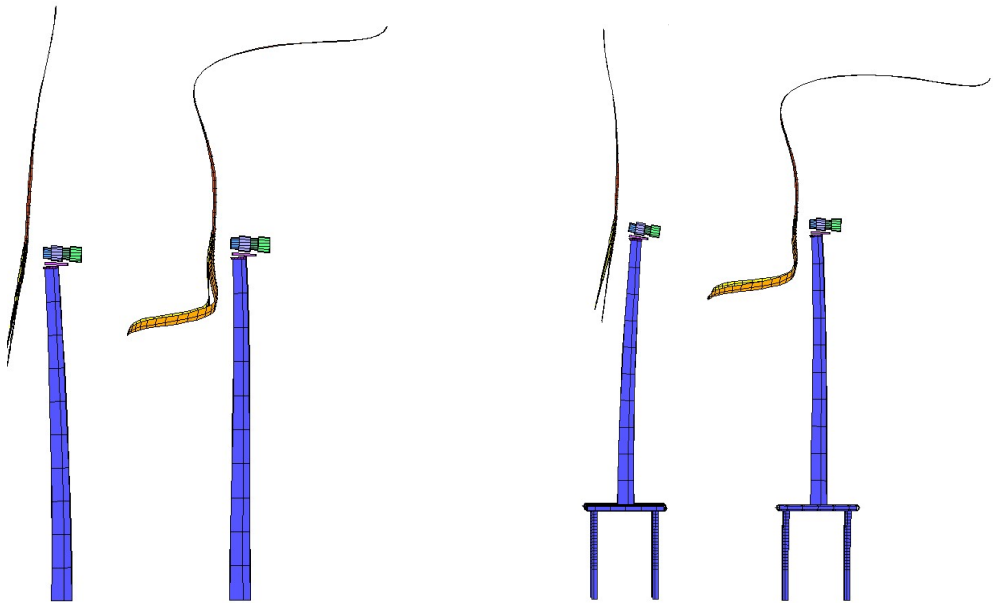

(a) (b)

Fig. 4. First and second FA support structure modes for (a) fixed foundation, (b) flexible foundation.

For both fixed and flexible foundation, Fig. 4 shows that the support structure modes involve, to a different extent, blade vibrations. On the other hand, previous studies have pointed out that blade modes play an important role in seismic response, as they may fall within the region of maximum spectral response acceleration [13]. Notice that rotor dynamics can be captured only by full models of the system, as those implemented in GH-BLADED [26] or similar codes [21], but is inevitably lost when simplified models with lumped mass modelling the RNA are adopted.

For the time-domain simulations described in Section 3, damping is set assuming the following structural modal damping ratios:

(a) fixed foundation: 0.4775% for blade modes and 1% for support structure modes, as in previous studies [12].

(b) flexible foundation: 0.4775% for blade modes and two different values, 5% and 20%, for support structure modes. In this case, the structural damping ratio of the support structure modes includes both material damping of the support structure and soil damping effects, as proposed in previous studies [40,41]. Typically, soil damping involve hysteretic and radiation damping, but estimates are rather difficult and affected by many factors, such as foundation geometry, soil characteristics and excitation frequencies; 5% and 20% may correspond to applications where soil damping contribution is estimated to be medium-low and high, respectively. They shall be taken only as potential structural modal damping ratios including both material damping of the support structure and soil damping, as different and even higher values may be considered [40,41,47].

2.2. Wind and earthquake loads

In GH BLADED [26], the aerodynamic loads on the spinning rotor are generated based on a dynamic wake model for the axial inflow, in conjunction with classical BEM model for the tangential inflow [48]. The dynamic wake model takes into account that changes in the blade loads affect the vorticity trailed into the rotor wake, and that the effect of these changes takes indeed a finite time to change the induced flow field, depending on which lift and drag forces acting on the blades are calculated [26].

The Kaimal spectrum is used for the wind process [29]:

$$S_k(f) = \frac{4\sigma_k^2 L_k/V}{(1+6f L_k/V)^{5/3}} \quad (1)$$

where f is the frequency (Hz), V is the wind velocity at hub height, k is the index referring to the velocity component (1 = X direction, 2 = Y direction and 3 = Z direction), σ_k is the standard deviation and L_k is the integral scale parameter of each velocity component, according to IEC 61400-1 prescriptions [29]. Wind is assumed to act in the X direction, and wind loads acting along the tower are included. Earthquake ground motion is modelled as an acceleration at the base with two horizontal components in X and Y directions.

In GH BLADED [26], the equations of motion are derived based on a multi-body dynamics approach combined with a modal representation of the flexible components, like blades and support structure. Within this framework, large displacements of the rotor with respect to the support structure are accounted for. The equations of motion are numerically integrated in the time-domain by the Runge-Kutta method, using a variable step.

3. COMPARISON BETWEEN FULLY-COUPLED AND UNCOUPLED ANALYSES

In this study, comparisons between combination of uncoupled analyses and fully-coupled simulation are made for earthquake striking in operational conditions, i.e. while the rotor is spinning. Both coupled and uncoupled analyses are implemented in the time domain, using GH BLADED [26] as follows.

Fully-coupled, nonlinear time-domain simulations are carried out by numerical integration of motion equations, considering mutual interactions of aerodynamic response and seismic response. That is, aerodynamic loads on the rotor blades are built taking into account blades motion due to global rotor motion and blades flexibility, as induced by wind loads, earthquake shaking at the base, control system etc.. The ground motion starts at t_0 = 400 s into the simulation, to ensure that the earthquake occurs as the system response has already attained a steady state [13,15,17]. After t_0 = 400 s, the simulation runs until the end of the earthquake record. Since the longest earthquake

record in this study lasts about 70 s (Chi-Chi Taiwan record, see Table 3), a total simulation length equal to 470 s is chosen and used, for simplicity, for all earthquake records [13,15].

In the uncoupled analyses, the separate responses to wind only and earthquake only are computed and then linearly combined. For wind excitation the rotor is spinning, while for earthquake excitation the rotor is considered in a parked state. Aerodynamic damping is considered when computing the separate response to earthquake only. In particular, consistently with numerical evidence on the seismic response of land-based HAWTs [10,18], the additional aerodynamic damping is included in the first two FA support structure modes, by suitably increasing the structural damping ratio assumed for the support structure modes (set equal to 1% for fixed foundation, 5% and 20% for flexible foundation, see Section 2.1). The simulation length for wind excitation is 470 s, i.e. identical to the length of the fully-coupled simulation, while the simulation length for earthquake excitation is 70 s, used for all earthquake records considered in this study for simplicity [13,15] (70 s = duration of the longest earthquake record in Table 3). The separate responses are linearly combined, summing the earthquake response to the wind response from the time instant at which the earthquake occurs in the fully-coupled simulation, i.e. t_0 = 400 s. The maxima SRSS bending-moment and shear-force at the tower base, encountered after t_0 = 400 s, are computed from the combined response, and compared with the corresponding value from the fully-coupled, nonlinear time-domain simulation, estimating the following errors:

$$M_r \text{ error} = \left(\frac{M_r - \bar{M}_r}{M_r} \right); \qquad F_r \text{ error} = \left(\frac{F_r - \bar{F}_r}{F_r} \right) \tag{2a,b}$$

$$\text{Total error: } \left(\frac{M_r - \bar{M}_r}{M_r} \right) + \left(\frac{F_r - \bar{F}_r}{F_r} \right) \tag{3}$$

In Eqs.(2)-(3), M_r and F_r are the maxima SRSS bending-moment and shear-force at the tower base obtained from the fully-coupled simulation, while $\bar{M}_r$ and $\bar{F}_r$ are the corresponding quantities from the combination of uncoupled analyses (subscripts x and y correspond to FA and SS directions in Fig. 2, respectively):

$$M_r = \sqrt{M_x^2 + M_y^2}; \quad F_r = \sqrt{F_x^2 + F_y^2} \tag{4a,b}$$

$$\bar{M}_r = \sqrt{\bar{M}_x^2 + \bar{M}_y^2}; \quad \bar{F}_r = \sqrt{\bar{F}_x^2 + \bar{F}_y^2} \tag{5a,b}$$

Uncoupled analyses will be implemented for various potential values of aerodynamic damping, and the comparison with the fully-coupled simulation will be carried out considering either error (2) or error (3). Comparisons of demands along the tower will also be made, as explained next.

4. NUMERICAL RESULTS

Ten real earthquake records and four wind velocities at the hub are considered, as in Table 3.

Wind and earthquake loading			
Earthquake records	Year	Station	PGA (m/s^2)
Cape Mendocino (CM)	1992	Petrolia	6.12
Chi Chi Taiwan (CC)	1999	TCU102	2.17
Erzican - Turkey (E)	1992	Erzican	4.43
Imperial Valley-06 (IV)	1979	E.C. #3	2.44
Irpinia - Italy 01 (I)	1980	Sturno	2.61
Kobe - Japan (K)	1995	KJMA	6.71
Landers (L)	1992	Lucerne	7.41
Morgan Hill (MH)	1984	G.A. #6	2.75
N. Palm Springs (NP)	1986	N.P.S	6.30
Northridge (N)	1994	P.D.d.	3.43
Wind velocities at the hub, V		No. of wind samples	
5 m/s		5	
11.4 m/s		5	
15 m/s		5	
20 m/s		5	

Table 3. Earthquake records and wind velocities at the hub.

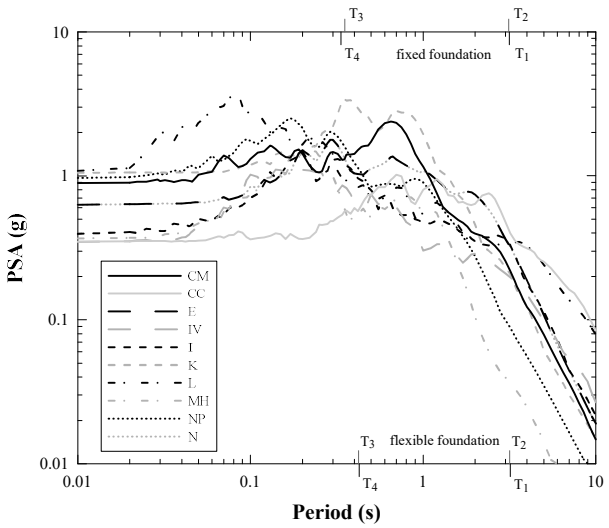

Fig. 5. 5% damped SRSS pseudo spectral acceleration for earthquake records in Table 3.

Earthquake records are chosen as they feature different peak ground acceleration and quite different frequency content [49], see Fig. 5 showing the 5% damped SRSS pseudo spectral acceleration (PSA) given in ref. [49] (= maximum SRSS of the 5% damped pseudo acceleration responses under the two earthquake horizontal components). In particular, horizontal components along X and Y in Fig. 2 coincide with first and second columns of the source files in ref. [49]. Records are not scaled to represent a specific site hazard, since the purpose here is to assess the accuracy of time-domain uncoupled analyses under a variety of peak ground accelerations.

Wind velocities are representative of potential operational states, within the cut-in-cut-out wind velocity range of the NREL 5MW HAWT (cut-in = 3.5 m/s and cut-out = 25 m/s, rated speed = 11.4 m/s, see Table 1). For each velocity, 5 wind samples are generated with 5 different seeds, to account for the inherent stochastic nature of the wind process. Wind samples are generated based on the Kaimal spectrum (1), assuming medium turbulence characteristics. All parameters in Eq.(1) are set according to IEC 61400-1 prescriptions for a normal turbulence model [29].

4.1. Fixed foundation

For the earthquake records, wind velocities V and wind samples in Table 3, Fig. 6 show the errors (2)-(3), as potential values of aerodynamic damping vary within the interval 0-8% at steps equal to 0.5%. In particular, 10×16=160 simulations have been run to compute the separate earthquake response for all potential aerodynamic damping values (10 ground motions, 16=8/0.5 potential aerodynamic damping values), 4×5=20 simulations to compute the separate wind response (5 samples for each of the 4 wind velocities), 10×4×5=200 fully-coupled simulations (10 ground motions, 5 samples for each of the 4 wind velocities), totaling 380 simulations. Fig. 6 reports the results of a few only, for brevity.

Results in Fig. 6 vary with earthquake records, wind velocities and samples of wind simulation. It is observed that, in most cases, an aerodynamic damping value capable of minimizing the total error (3) may be found. Typically, these are the cases in which either the "M_r error" (2a), or both "M_r error" (2a) and "F_r error" (2b), start from negative values for the lowest aerodynamic damping

0.5% and progressively tend to zero as aerodynamic damping increases. That is, the combination of uncoupled analyses provides larger demands than the fully-coupled simulation for the lowest aerodynamic damping 0.5% ("M_r error" < 0 means $\bar{M}_r > M_r$, "F_r error" < 0 means $\bar{F}_r > F_r$), and progressively approaches the fully-coupled simulation with increasing aerodynamic damping. However, there may also be cases in which no minimum is found for the total error (3). In general, this occurs when both "M_r error" (2a) and "F_r error" (2b) start from positive values for the lowest aerodynamic damping 0.5%, and monotonically increase as aerodynamic damping increases. In these cases, $\bar{M}_r$ and $\bar{F}_r$ from the combination of uncoupled analyses are always smaller than M_r and F_r from fully-coupled simulation, regardless of the aerodynamic damping values. Such result is not surprising, since ref. [31] had already shown that the combination of separate wind and earthquake responses, the latter being computed with the inclusion of aerodynamic damping, may provide smaller bending-moment demands with respect to fully-coupled simulations [31] (no results are reported in ref. [31] on shear-force demands), and is explained considering that any aerodynamic damping based approach is, indeed, an approximate approach to account for the inherently nonlinear interaction between aerodynamic and seismic responses (e.g. see Fig. 13 in ref. [31]). At any rate, based on the results in Fig. 6, it can be concluded that an aerodynamic damping level minimizing the difference between fully-coupled simulation and combination of uncoupled analyses, in terms of the total error (3) involving both bending-moment and shear-force demands at the tower base, cannot exist for all ground motions and wind samples in Table 3.

Once it is established that such an aerodynamic damping value cannot exist, attention is focused on bending-moment and shear-force errors (2) at the tower base when, in the combination of uncoupled analyses, the separate earthquake response is built with a 4% aerodynamic damping. Fig. 7 shows that errors (2) are generally below 10%, with a few maxima values almost equal to 20%, for all the considered ground motions and wind samples. The errors can be considered acceptable from an engineering point of view, and in agreement with errors encountered in alternative formulations of uncoupled analyses in the literature, as for instance the SRSS combination of separate wind and earthquake responses computed by the IEC method [17], which provide errors up

to 20% depending on the PSA (see Figure 8.11 in ref. [17]). Also, as earlier mentioned, the fact that errors (2) may be negative or positive appears consistent with previous results in ref. [17,31], which showed that the combination of uncoupled analyses does not necessarily provides always conservative results with respect to fully-coupled simulation (see Figure 8.11 in ref. [17] or Fig. 13 in ref. [31]).

For an insight into the results in Fig. 7, Fig. 8 reports the time histories of SRSS bending moment and shear force at the tower base, as obtained from fully-coupled simulation and combination of uncoupled analyses with 4% aerodynamic damping in the separate earthquake response, under Northridge earthquake record and a wind realization for V=11.4 m/s at the hub (only the time history above t_0=400 s is reported, for brevity). A good matching is observed between the two methods. Results for other earthquake records/wind realizations in Table 3 are similar to those in Fig. 8 and are omitted here, for brevity.

For a further validation of the results obtained with a 4% aerodynamic damping, Figs. 9-10 show the mean of SRSS bending-moment and shear-force demands along the tower, as computed by the combination of uncoupled analyses and fully-coupled simulation. For each wind velocity and ground motion, the mean is obtained by averaging the demands from all wind realizations. Errors in Figs. 9-10 can generally be considered within engineering margins along the whole tower. It is interesting to remark that the errors in the mean bending-moment demands in Fig. 9 are similar to those obtained by Asareh and Prowell [31], who used a 0.75 combination factor to combine the operational wind demand and the earthquake demand computed with a 4% aerodynamic damping.

At this stage, based on the results in Fig. 7 through Fig. 10 for fixed foundation, it can be concluded that the combination of time-domain uncoupled analyses, with 4% aerodynamic damping in the separate earthquake response, can provide a reasonable estimate of maxima and mean demands from fully-coupled simulations. It is remarkable that such a level of aerodynamic damping agrees with the one recommended by ASCE-AWEA RP2011 [30] for combining uncoupled analyses, where the separate earthquake response is computed by a response-spectrum approach. The same level of aerodynamic damping was also used in previous studies [25,27,31], as discussed in the Introduction.

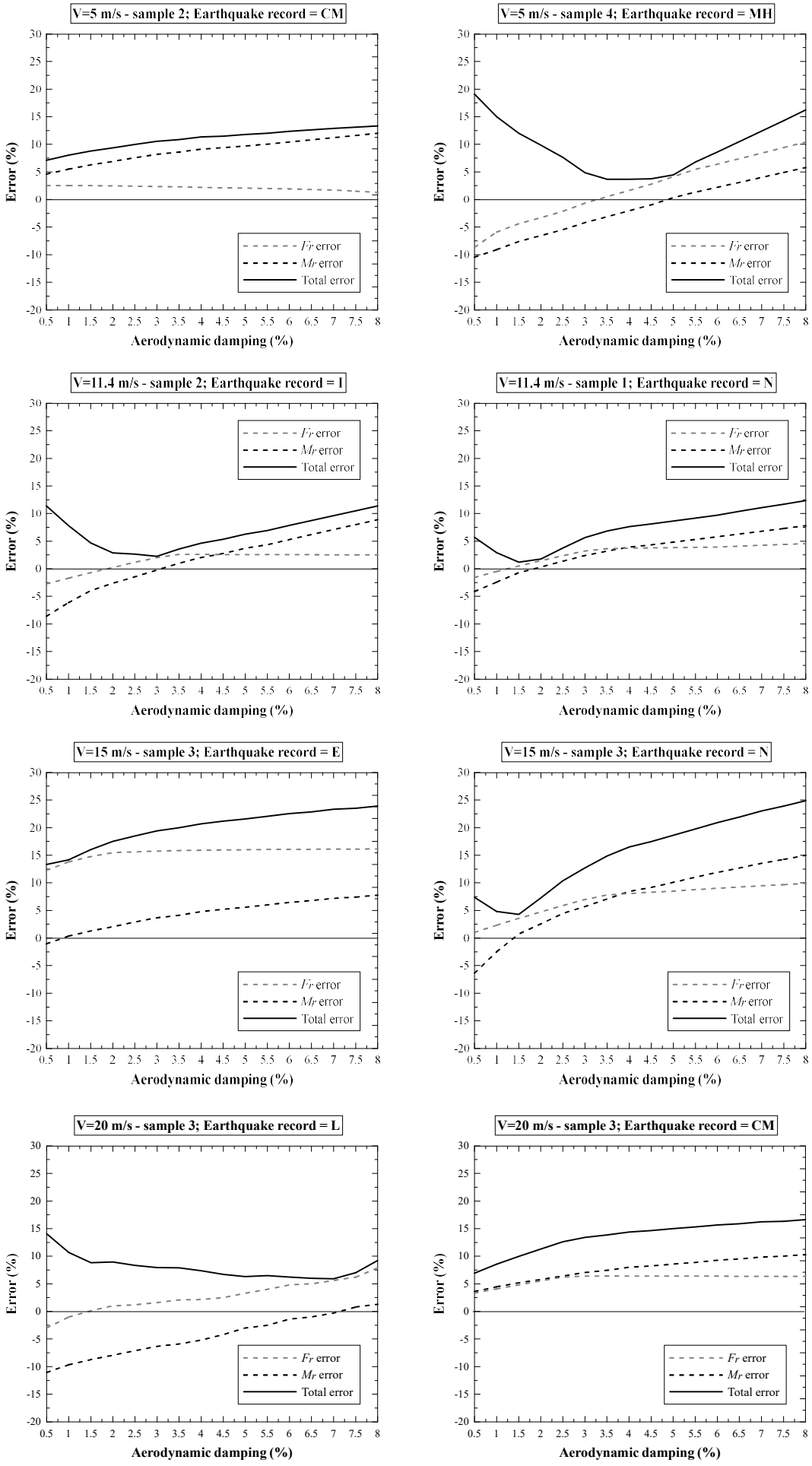

Fig. 6. Fixed foundation: Errors (2)-(3) for various potential aerodynamic damping values, under various earthquakes in Table 3.

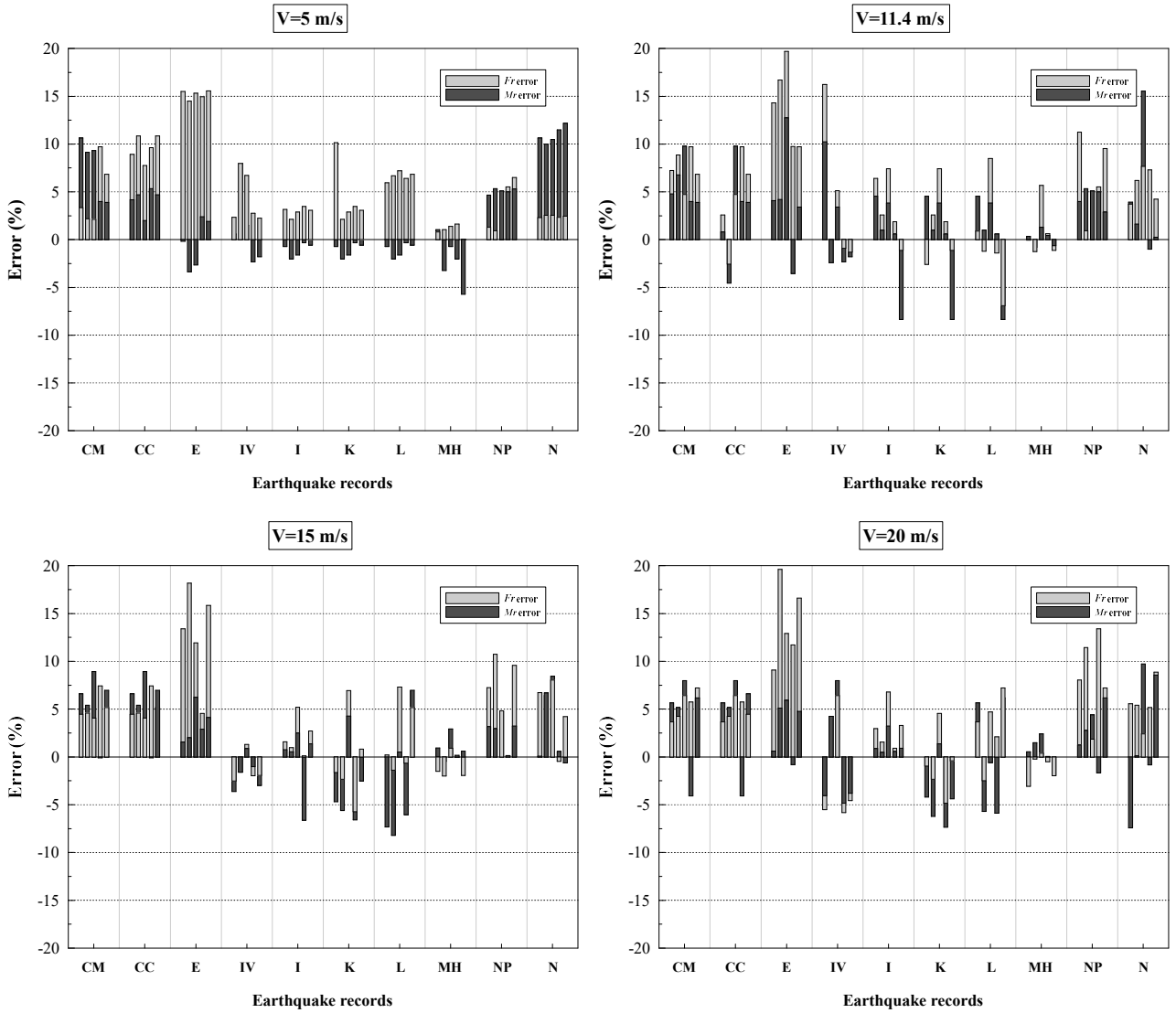

Fig. 7. Fixed foundation: Errors (2) for 4% aerodynamic damping, under all earthquakes in Table 3.

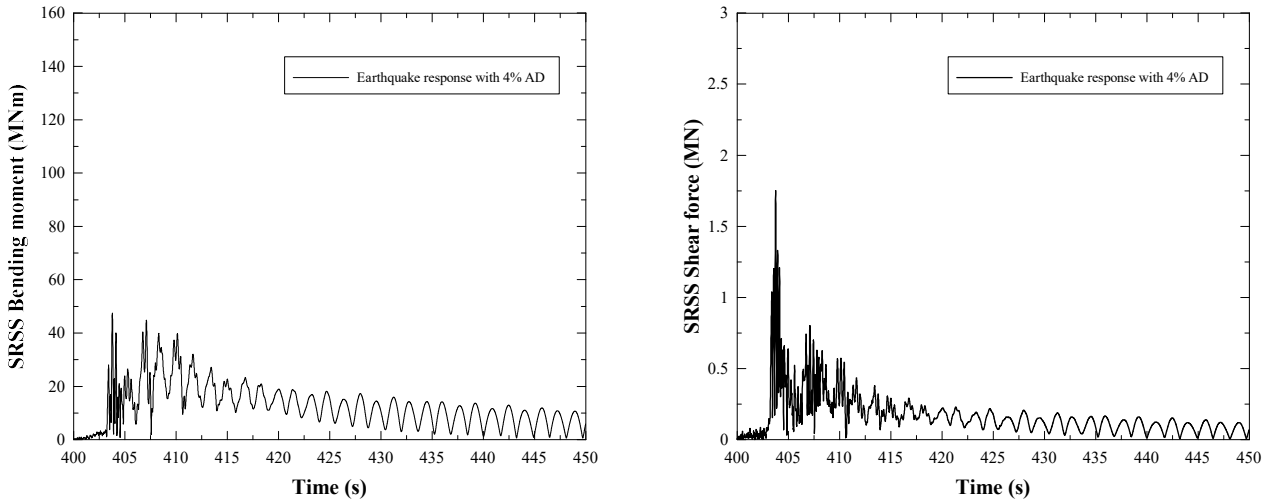

(a)

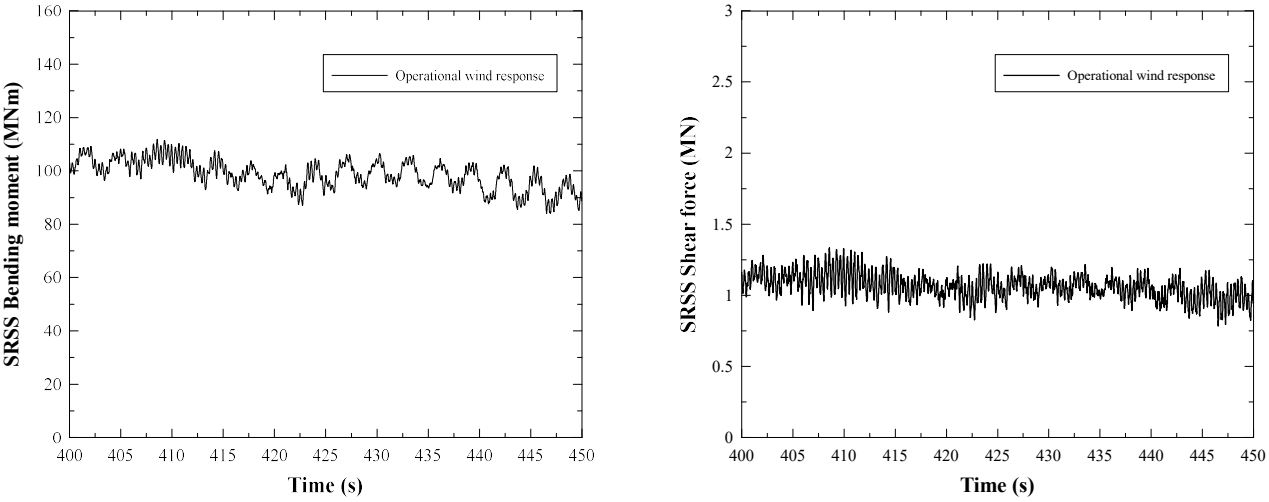

(b)

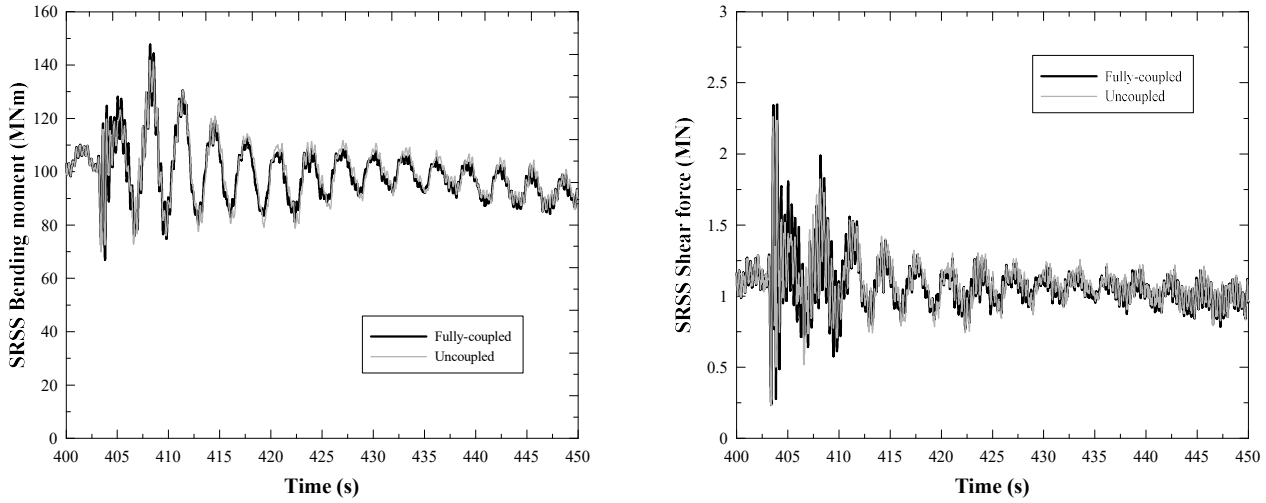

(c)

Fig. 8. Fixed foundation: SRSS bending moment and shear force at the tower base under Northridge earthquake and a wind sample for V=11.4 m/s at the hub; (a) earthquake response with 4% aerodynamic damping (AD), (b) operational wind response, (c) comparison between fully-coupled simulation and combination of uncoupled analyses, with a 4% aerodynamic damping in the earthquake response.

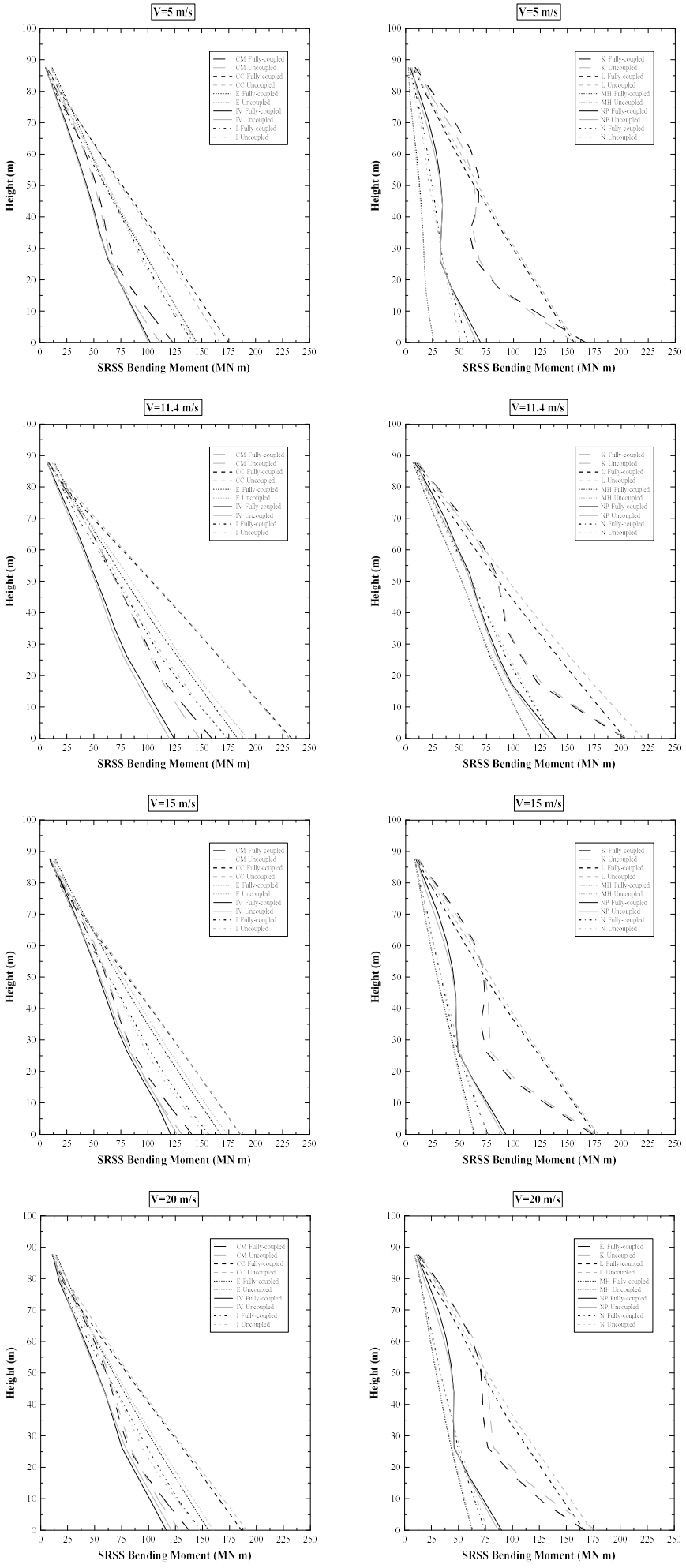

Fig. 9. Fixed foundation: mean bending-moment demands along the tower, for all earthquakes in Table 3.

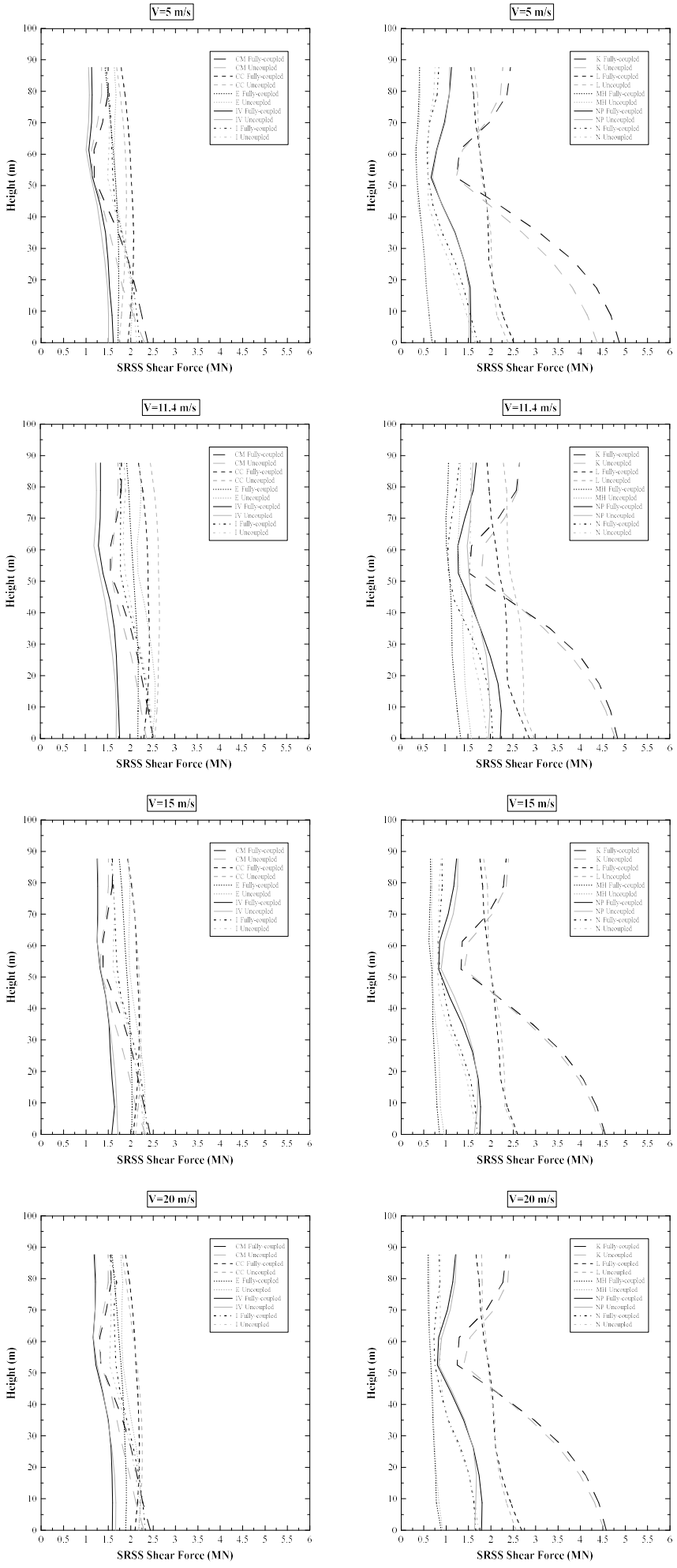

Fig. 10. Fixed foundation: mean shear-force demands along the tower, for all earthquakes in Table 3.

A final remark is in order. The advantage of the proposed uncoupled analyses is that the wind response, once computed for a given sample of wind velocity at the hub, applies for any earthquake record. The fully-coupled simulation, instead, must be re-run whenever the earthquake record changes. In view of the simulation length set in Section 3, this means that, for a given sample of wind velocity:

(i) The uncoupled-analyses approach requires 1 wind response simulation (470 s) + 10 earthquake response simulations (70 s each), totaling 470 + 10×70 = 1170 s simulation time.

(ii) The fully-coupled simulation approach requires 10 wind-earthquake simulations (470 s each), totaling 10×470 = 4700 s simulation time.

Obviously, the computational advantage becomes particularly relevant when several responses have to be compared for various potential earthquake realizations, as is typical in a design process.

4.2. Flexible foundation

As earlier mentioned in the Introduction, the major interest in implementing time-domain uncoupled analyses for seismic assessment of land-based HAWTs is that, in the time domain, sources of nonlinearity due, for instance, to foundation modeling, can readily be accounted for in the structural model. In contrast, this is not possible in uncoupled analyses where the separate earthquake response is computed by a response-spectrum approach, because in this case modal periods shall necessarily be computed from a linear or linearized structural model. For instance, a linearization requiring an iterative procedure was proposed in ref. [7], to study the earthquake response of a parked HAWT on a surface footing.

Here, the feasibility of time-domain uncoupled analyses including the flexible nonlinear-spring foundation in Section 2 will be investigated, following the approach described in Section 4.1 for fixed foundation. Soil damping effects are accounted for by setting, for the support structure modes, structural damping ratios equal to 5% or 20% (see Section 2.1). Results for 5% structural damping will be discussed in this Section. It will be seen that results for 20% structural damping mirror those for 5% structural damping and, for brevity, they will be reported in Appendix A.

Fig. 11 shows errors (2)-(3) as potential aerodynamic damping varies within the interval 0-8% at step 0.5%, for the earthquake records, wind velocities and wind samples in Table 3, when a 5% structural damping ratio is considered in the support structure modes. As in Section 4.1, 380 simulations have been run (10×16=160 separate earthquake responses + 4×5=20 separate wind responses + 10×4×5=200 fully-coupled simulations), and only a few results are reported for brevity. Results mirror those in Fig. 6. In most cases, an aerodynamic damping value minimizing the total error (3) may be found, typically when the combination of uncoupled analyses provide larger demands than the fully-coupled simulation for the lowest aerodynamic damping 0.5%, and progressively approach the fully-coupled simulation as aerodynamic damping increases. In some cases, however, an aerodynamic damping value minimizing the total error (3) is not found, as the combination of uncoupled analyses provide smaller values than the fully-coupled simulation regardless of the aerodynamic damping value. As in the case of fixed foundation, therefore, it shall be concluded that an aerodynamic damping value capable of minimizing the total error (3) cannot exist.

Fig. 12 shows the shear-force and bending-moment errors (2), when a 4% aerodynamic damping is considered to compute the separate earthquake response. Again, results agree with those in Fig. 7 for fixed foundation. In most cases, errors are below 10%, with a few maxima values around 15%. Thus, errors are within the engineering margins encountered in existing combinations of uncoupled analyses, see the SRSS combination of separate wind and earthquake responses computed by the IEC method [17] (Figure 8.11 in ref. [17]). For a further validation, Figs. 13-14 show the mean SRSS bending-moment and shear-force demands computed over all wind samples for each wind velocity and ground motion, as obtained by combination of uncoupled analyses and fully-coupled simulation. Results appear quite accurate along the whole tower. In particular, errors in the mean bending-moment demands agree with those found by Asareh and Prowell in ref. [31], who used a 0.75 factor to combine the separate operational wind demand and the separate earthquake demand computed with a 4% aerodynamic damping.

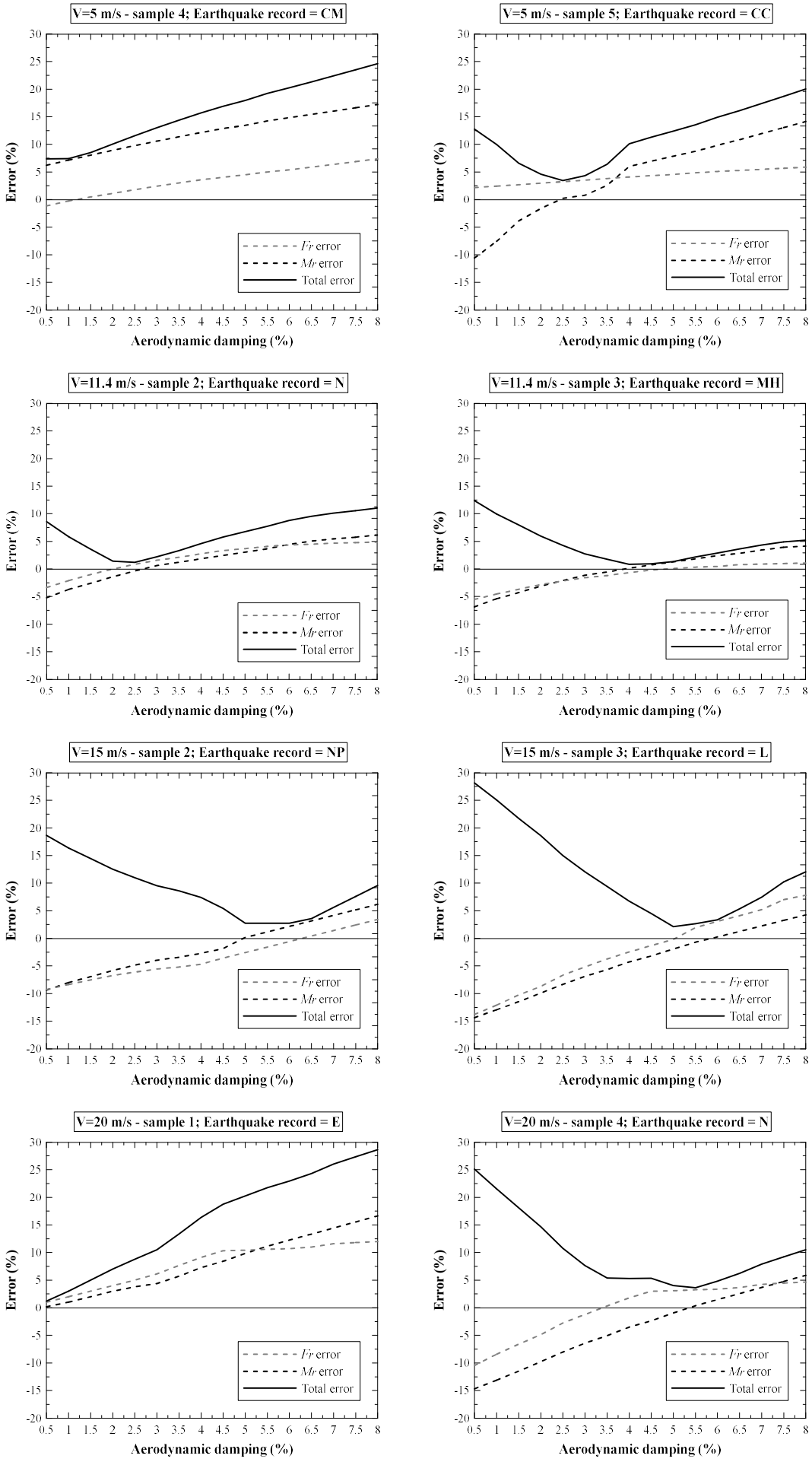

Fig. 11. Flexible foundation with 5% structural damping ratio in support structure modes: Errors (2)-(3) for various potential aerodynamic damping values, under various earthquakes in Table 3.

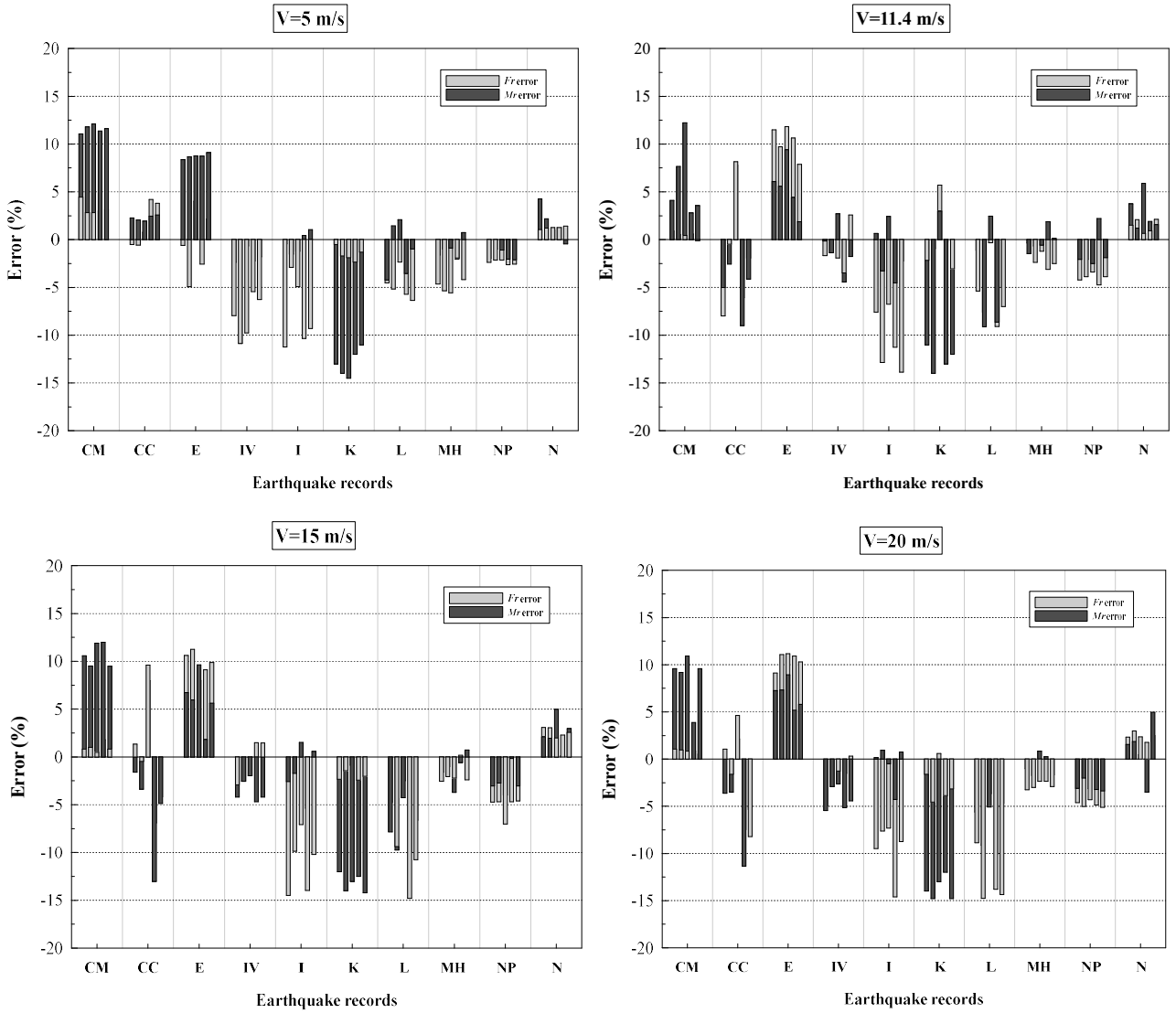

Fig. 12. Flexible foundation with 5% structural damping ratio in support structure modes: Errors (2) for 4% aerodynamic damping, under all earthquakes in Table 3.

Based on the results in Fig. 12 through Fig. 14, therefore, it can be concluded that a 4% aerodynamic damping may be used also in the combination of time-domain uncoupled analyses, which involve the nonlinear-spring foundation model in Section 2. Again, it is remarkable that such a level of aerodynamic damping agrees with that recommended by ASCE-AWEA RP2011 [30] for uncoupled analyses with separate earthquake response computed by a response-spectrum approach, and used also in previous studies [25,27,31].

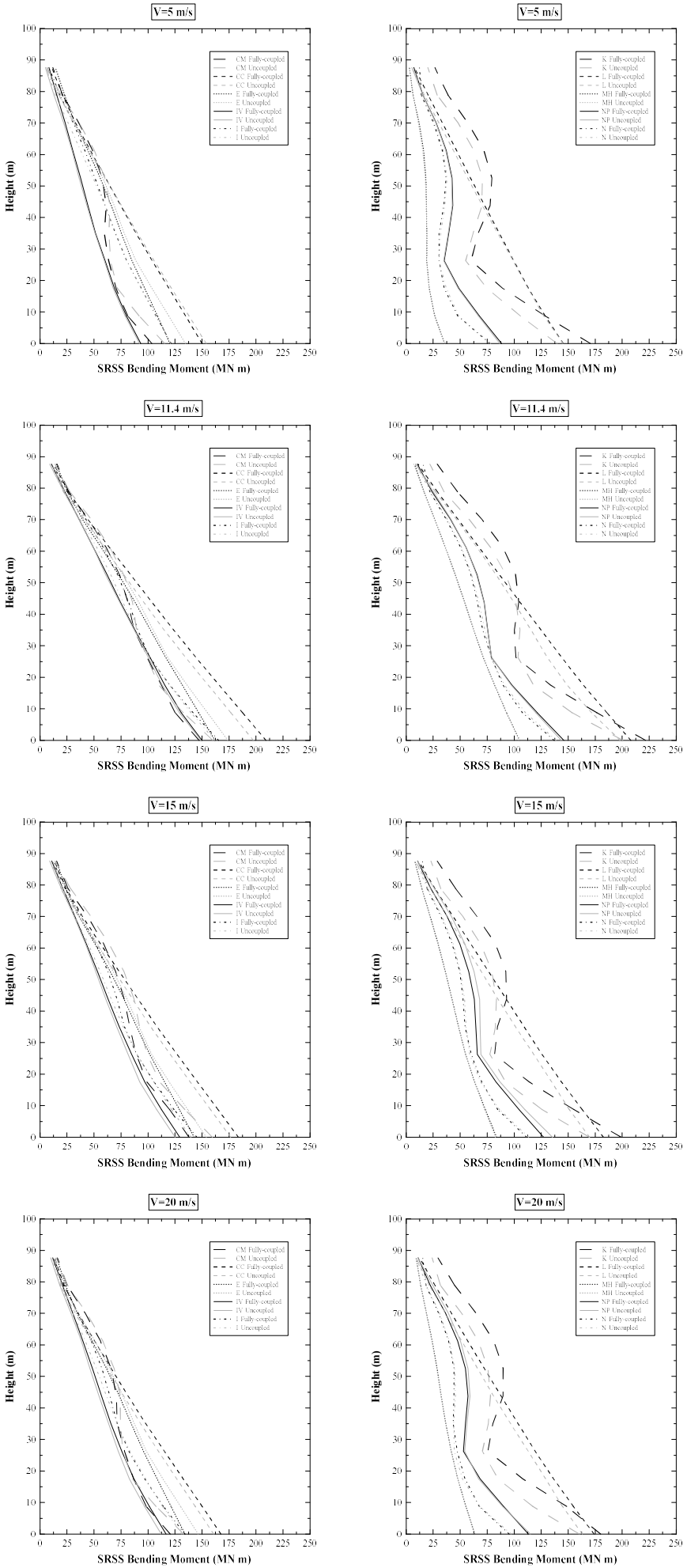

Fig. 13. Flexible foundation with 5% structural damping ratio in support structure modes: mean bending-moment demands along the tower, for all earthquakes in Table 3.

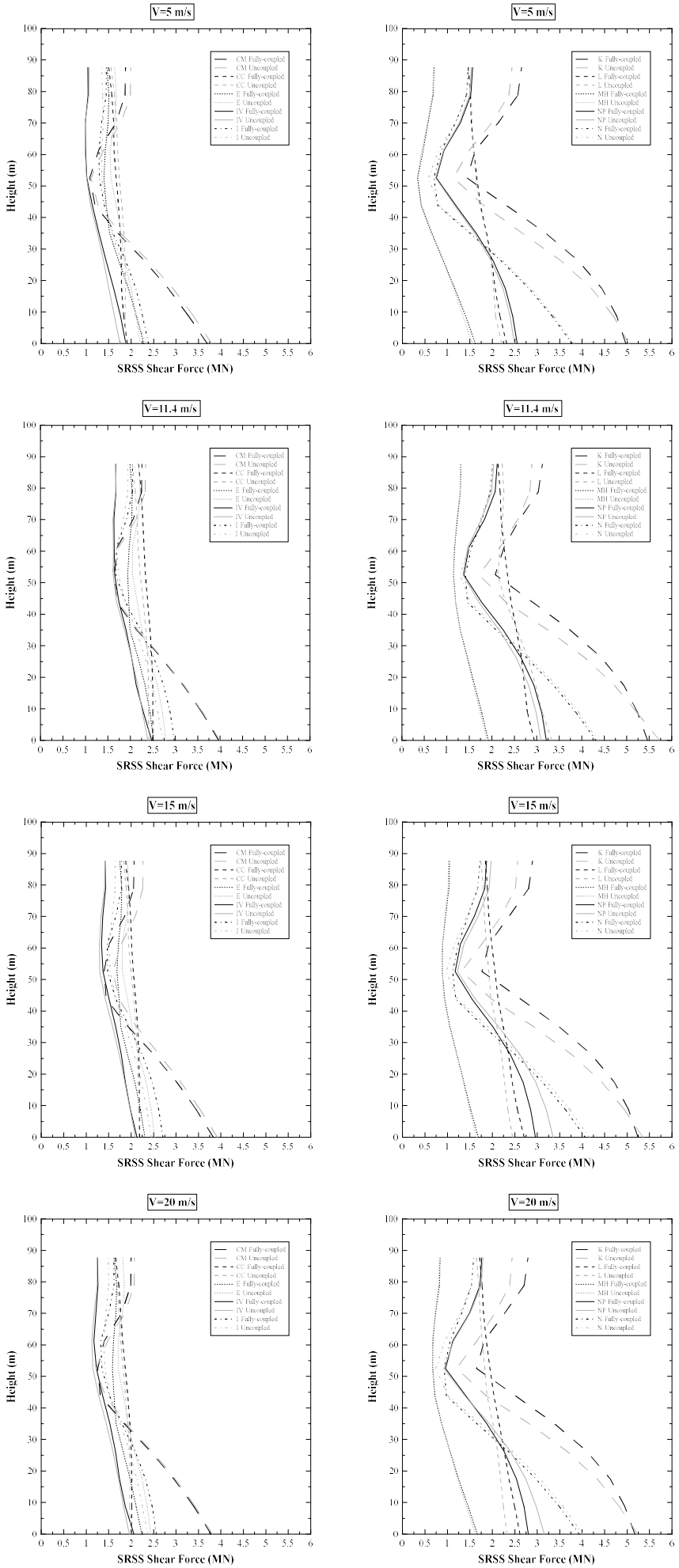

Fig. 14. Flexible foundation with 5% structural damping ratio in support structure modes: mean shear-force demands along the tower, for all earthquakes in Table 3.

At this stage, a few further comments are in order.

The first is that bending-moment and shear-force demands for fixed and flexible foundations are within the same range, see Figs. 9-10 and Figs. 13-14. This reflects the fact that, as shown in Fig. 5, periods of the first FA and SS support structure modes are practically the same for fixed and flexible foundations, and periods of the second FA and SS support structure modes for flexible foundation, although smaller than the corresponding ones for fixed foundation, still fall within the regions of high acceleration in the response spectrum (see again Fig. 4). In general, therefore, both fixed and flexible foundation models shall be investigated, when searching for most unfavorable conditions for seismic design of HAWTs.

A second relevant comment concerns nonlinear effects in the foundation. For each wind velocity and ground motion, and some of the wind samples in Table 3, Fig. 15 shows the maxima lateral x-deflections along pile #1 (see Fig. 2), as obtained from fully-coupled simulation and combination of uncoupled analyses. Results from the two methods are in satisfactory agreement over the whole pile. In addition, Fig. 15 includes the lateral x-deflections corresponding to a 25% deviation from the initial tangent in the p-y API curves [32] at various depths, for the considered sandy soil. Here, such lateral deflections are taken as indicators of a significant nonlinear soil response. It is observed that nonlinear effects are considerable over about one fourth of the total pile length. These results suggest that using linearized p-y curves may not be appropriate for seismic assessment, and substantiate the interest in time-domain uncoupled analyses, which may include nonlinear foundation behaviour directly in the structural model, as proposed in this study. Similar results are found for the other wind samples, and are omitted for brevity.

Results for 20% structural damping ratio in the support structure modes, to account for soil damping effects, may be found in Appendix A. Comments and observations mirror those made on Fig. 11 through Fig. 14 of this Section, and are omitted for conciseness.

Finally, it is worth remarking that computational advantages of the proposed uncoupled analyses hold for fixed as well as flexible foundation. They have been discussed in Section 4.1 and are not repeated here.

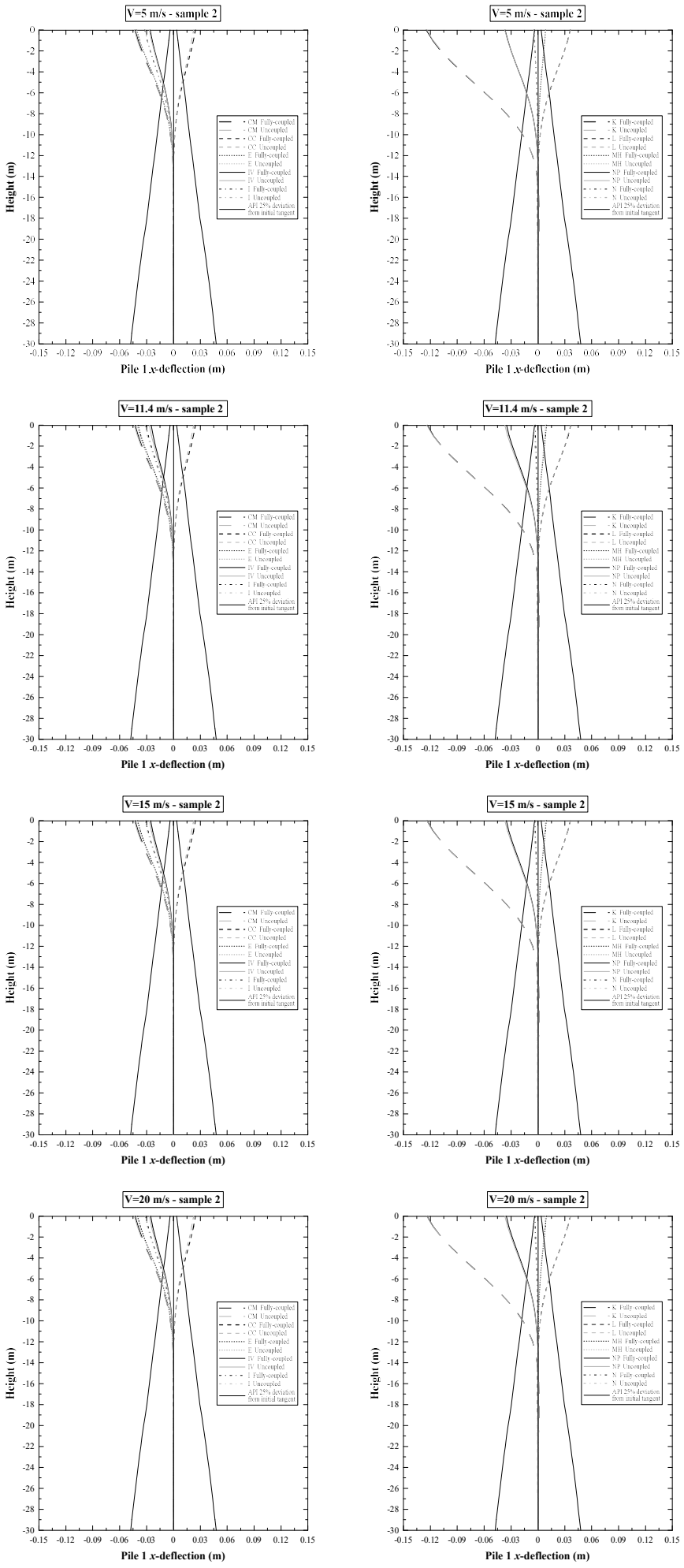

Fig. 15. Flexible foundation with 5% structural damping ratio in support structure modes: maxima *x*-deflections along pile #1, for some wind samples in Table 3.

5. CONCLUSIONS

The present study has proposed a time-domain implementation of uncoupled analyses for seismic assessment of land-based HAWTs, in operating conditions. Wind and earthquake responses are separately computed and linearly superposed, with the earthquake response computed from a structural model where additional aerodynamic damping is introduced. Unlike existing response-spectrum based uncoupled analyses, the proposed time-domain implementation allows nonlinear foundation behavior to be readily included in the structural model.

The NREL 5MW baseline HAWT, mounted on a column with a pile-supported square footing, has been considered as case study. Uncoupled analyses have been implemented on a full model of the system in GH BLADED [26], and compared with fully-coupled simulations. It has been shown that, when the separate earthquake response is computed using a 4% aerodynamic damping, reasonably accurate results can be obtained in terms of shear-force and bending-moment demands, with errors in maxima and mean demands similar to those obtained from uncoupled analyses existing in the literature [17,31]. It is remarkable that a 4% aerodynamic damping is also recommended by ASCE-AWEA RP2011 [30] for response-spectrum based uncoupled analyses, and is in agreement with previous studies [25,27,31]. This result has been obtained for both fixed and flexible foundation, with the latter modeled by nonlinear springs set from API code [32] and soil damping included in the structural damping ratio of the support structure modes. Specifically, 5% and 20% structural damping ratios have been considered for such modes. It has been found that earthquake ground motion may induce a significantly nonlinear response at the foundation level, substantiating the need for implementing time-domain uncoupled analyses, where nonlinear foundation behavior may be directly included in the structural model.

Further work is certainly needed to investigate the proposed approach for wind turbines with different sizes and operational characteristics, alternative *p-y* curves [38-39, 42-46], different types of foundation and pertinent models [50-52]. Also, of particular interest is the feasibility of analogous time-domain uncoupled analyses for seismic assessment of offshore HAWTs [53,54].

APPENDIX A

This Appendix contains the results obtained for flexible foundation model, when a 20% structural damping ratio is assumed in the support structure modes. As explained in Section 2.1, such structural modal damping ratio accounts for both material damping of the support structure and soil damping effects, in accordance with previous studies on the dynamic response of pile-supported offshore wind turbines under dynamic loads [40,41].

Figures in this Appendix are presented following the outline of Section 4.2. Results confirm that the combination of time-domain uncoupled analyses, with 4% aerodynamic damping in the separate earthquake response, provides a reasonable estimate of maxima and mean demands from fully-coupled simulations. Errors are indeed within the same engineering margins observed for fixed foundation, and flexible foundation with 5% structural damping ratio in the support structure modes. It is noticed that bending-moment and shear-force demands along the tower, shown in Figs. 18-19, are generally smaller than those in Figs. 9-10 (fixed foundation) and Figs. 13-14 (flexible foundation with 5% structural damping ratio in the support structure modes). Obviously, this is attributable to the increased damping in the support structure modes. Likewise, maxima deflections along pile #1 are slightly smaller than those in Fig. 15.

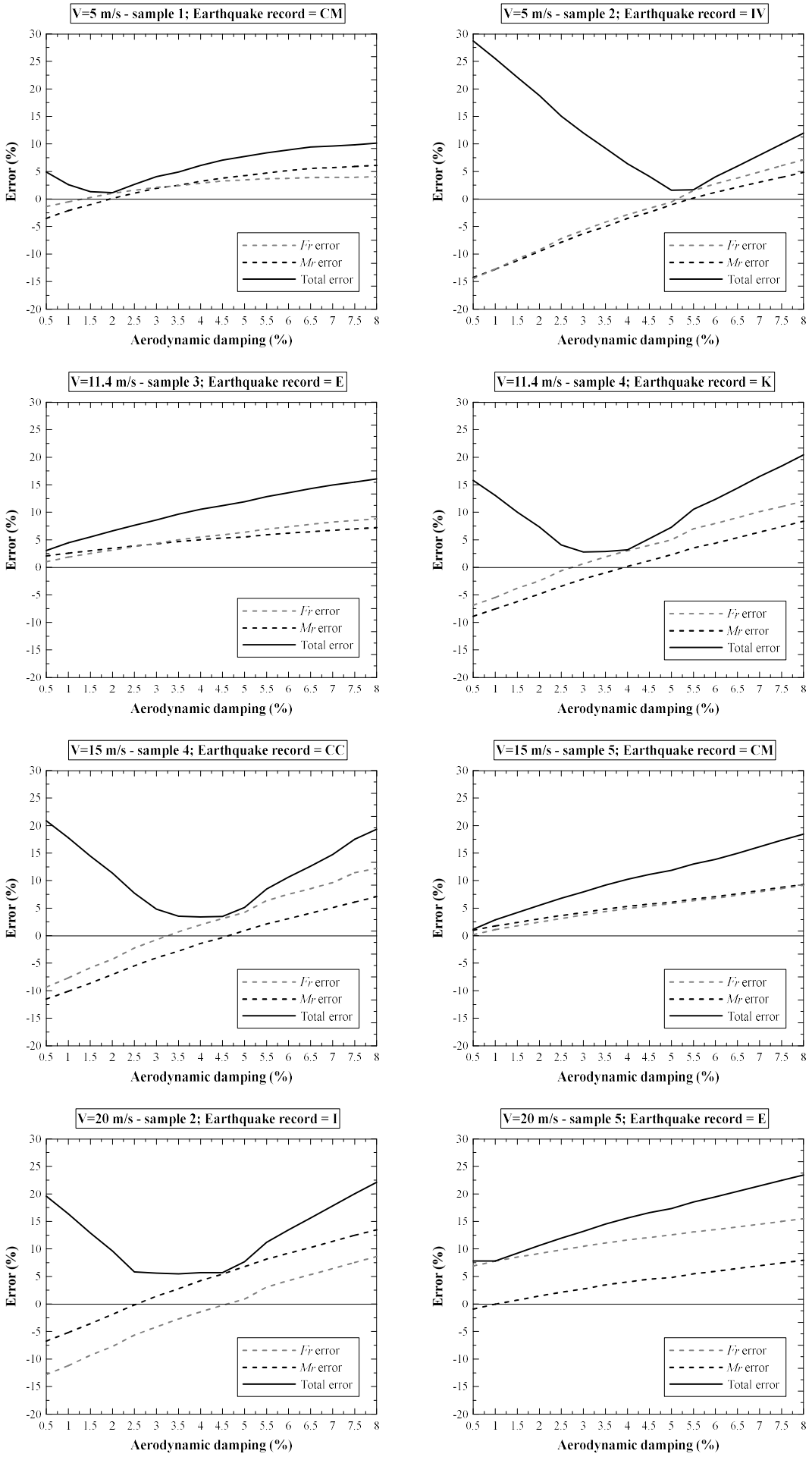

Fig. 16. Flexible foundation with 20% structural damping ratio in support structure modes: Errors (2)-(3) for various potential aerodynamic damping values, under various earthquakes in Table 3.

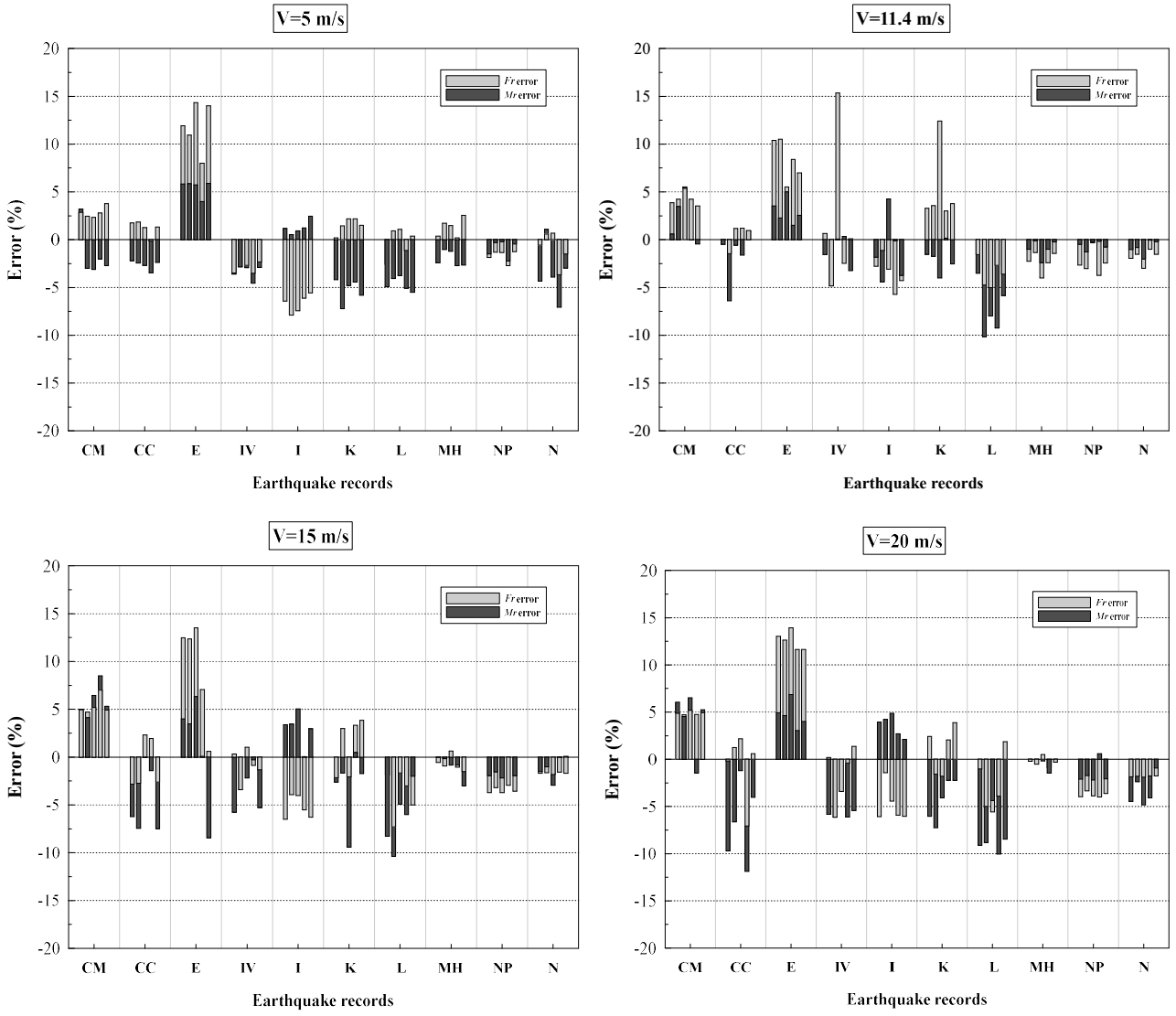

Fig. 17. Flexible foundation with 20% structural damping ratio in support structure modes: Errors (2) for 4% aerodynamic damping, under all earthquakes in Table 3.

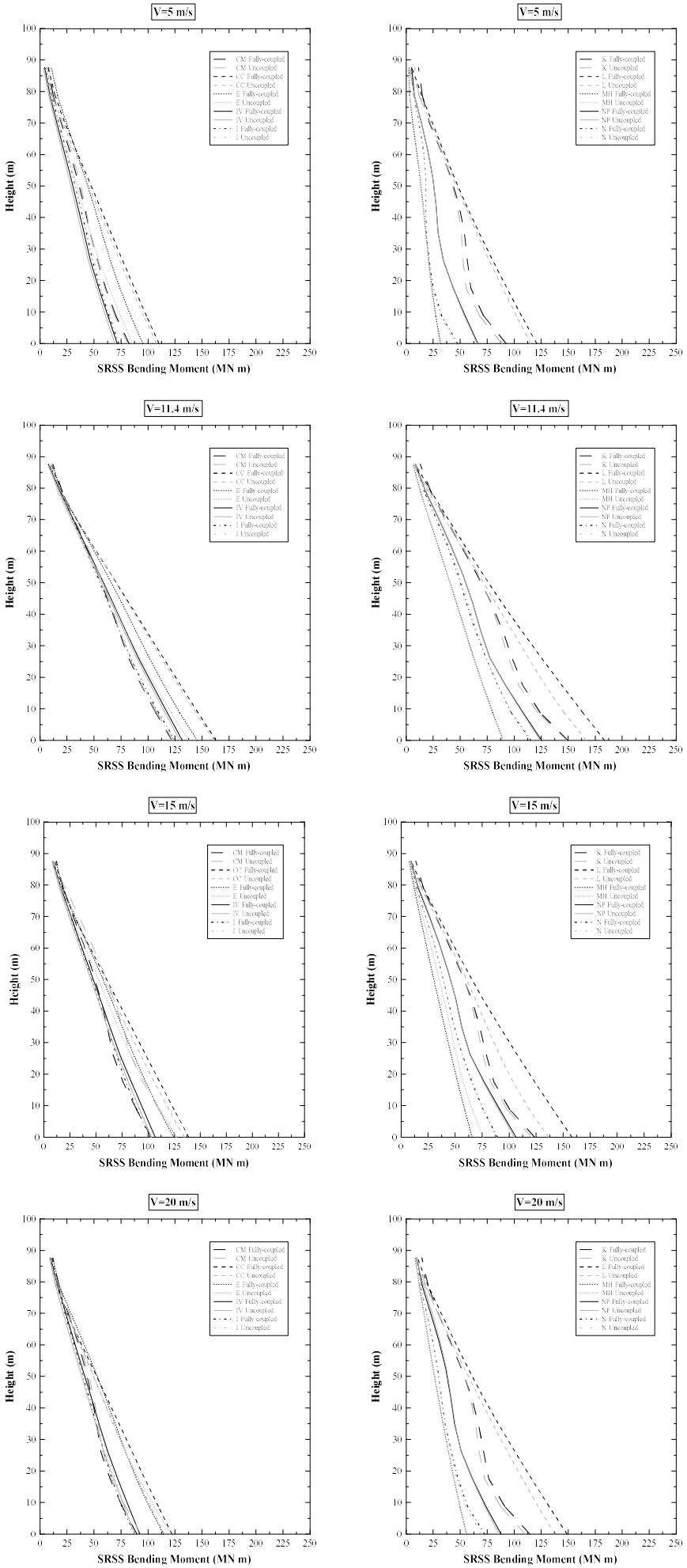

Fig. 18. Flexible foundation with 20% structural damping ratio in support structure modes: mean bending-moment demands along the tower, for all earthquakes in Table 3.

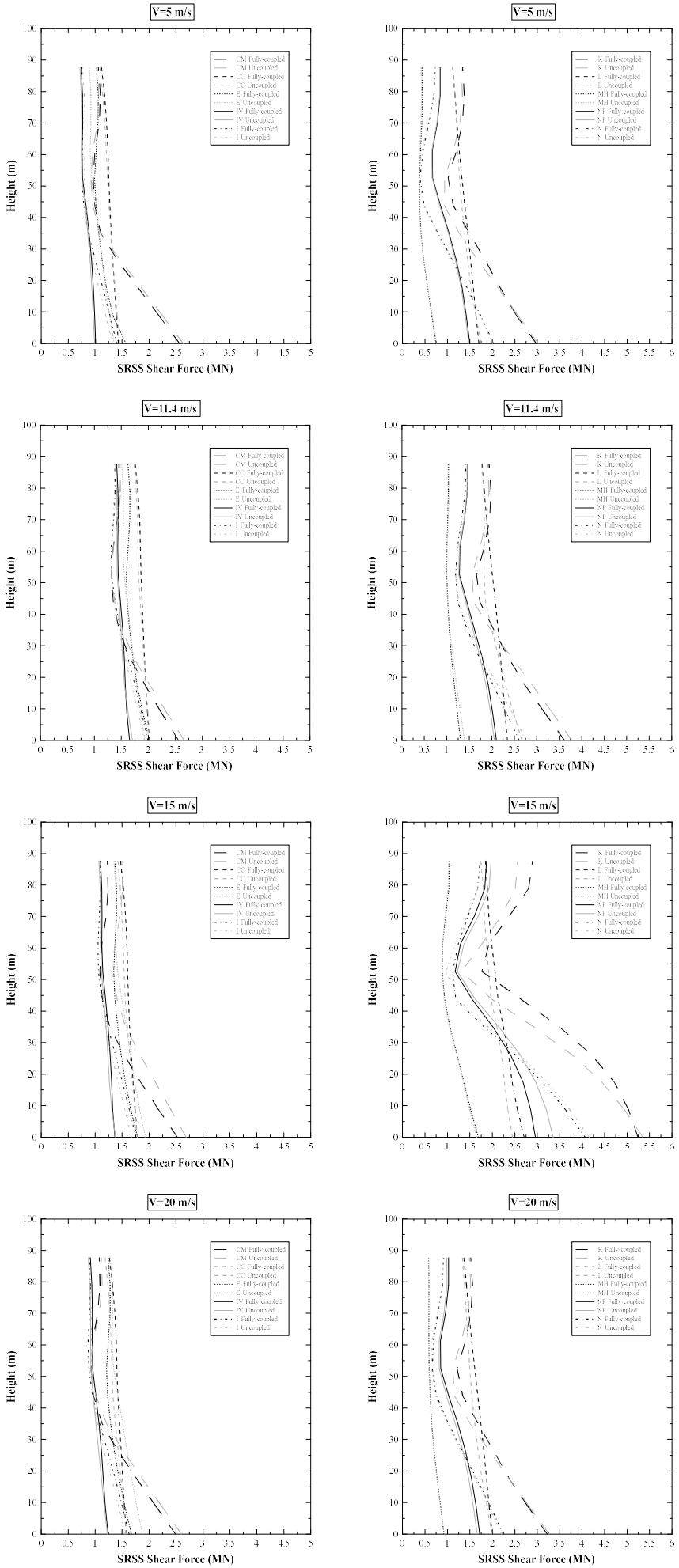

Fig. 19. Flexible foundation with 20% structural damping ratio in support structure modes: mean shear-force demands along the tower, for all earthquakes in Table 3.

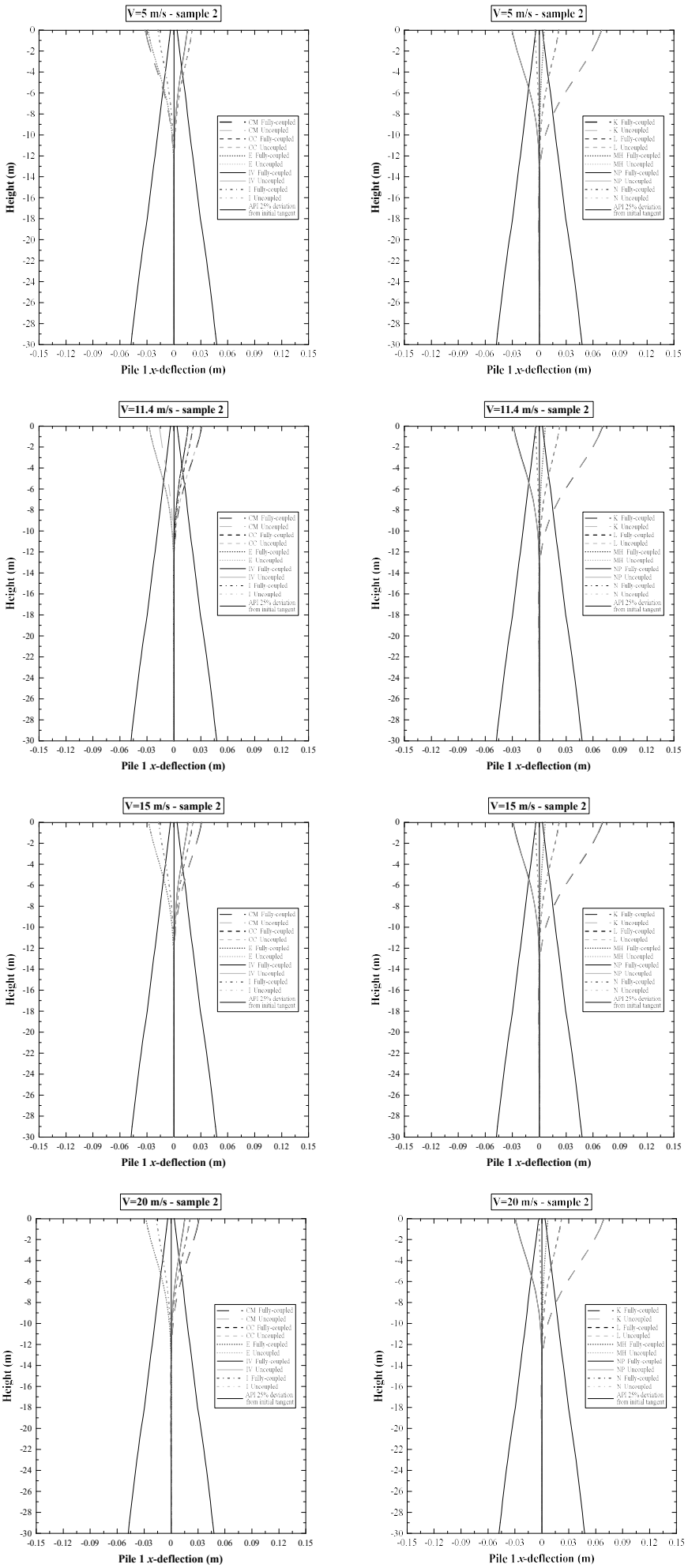

Fig. 20. Flexible foundation with 20% structural damping ratio in support structure modes: maxima *x*-deflections along pile #1, for some wind samples in Table 3.

REFERENCES

[1] Global Wind Energy Council (GWEC). Global wind report: Annual market update 2014. Brussels: Global Wind Energy Council; 2015.

[2] U.S. Department of Energy (DOE). 2014 Wind technologies market report. Oak Ridge: U.S. Department of Energy; 2015.

[3] Prowell I, Veers P. Assessment of wind turbine seismic risk: existing literature and simple study of tower moment demand. Technical Report No. SAND2009-1100. Albuquerque: Sandia National Laboratories; 2009.

[4] Failla G. Seismic analysis of wind energy converters. In: Beer M, Kougioumtzoglou IA, Patelli E, Au IS-K, editors. Encyclopedia of earthquake engineering. Berlin-Heidelberg: Springer-Verlag; 2014.

[5] Bazeos N, Hatzigeorgiou GD, Hondros ID, Karamaneas H, Karabalis DL, Beskos DE. Static, seismic and stability analyses of a prototype wind turbine steel tower. Eng Struct 2002; 24:1015-1025.

[6] Lavassas I, Nikolaidis G, Zervas P, Efthimiou E, Doudoumis IN, Baniotopoulos CC. Analysis and design of the prototype of a steel 1-MW wind turbine tower. Eng Struct 2003; 25(8): 1097-1106.

[7] Stamatopoulos GN. Response of a wind turbine subjected to near-fault excitation and comparison with the Greek Aseismic Code provisions. Soil Dyn Earthq Eng 2013; 46: 77-84.

[8] Mulliken JS, Karabalis DL. Discrete models for through-soil coupling of foundations and structures. Earthq Eng Struct Dyn 1998; 27:687-710.

[9] Sapountzakis EJ, Dikaros IC, Kampitsis AE, Koroneou AD. Nonlinear response of wind turbines under wind and seismic excitations with soil-structure interaction. J Comput Nonlinear Dyn 2015; 10: 041007.

[10] Díaz O, Suárez LE. Seismic analysis of wind turbines. Earthq Spectra 2014; 30(2): 743-765.

[11] Asareh MA. Dynamic behavior of operational wind turbines considering aerodynamic and seismic load interaction. PhD dissertation, Missouri University of Science and Technology; 2015.

[12] Jonkman JM, Butterfield S, Musial W, Scott G. Definition of a 5-MW reference wind turbine for offshore system development. Technical Report No. NREL/TP-500-38060. Golden: National Renewable Energy Laboratory; 2009.

[13] Prowell I, Elgamal A, Uang C, Jonkman J. Estimation of seismic load demand for a wind turbine in the time domain. In: Proceedings of the European Wind Energy Conference (EWEC), Warsaw, Poland, 20-23 April 2010.

[14] Laino DJ, Hansen AC. User's guide to the wind turbine aerodynamics computer software AeroDyn, Windward Engineering, 2002.

[15] Asareh MA, Schonberg W, Volz J. Effects of seismic and aerodynamic load interaction on structural dynamic response of multi-megawatt utility scale horizontal axis wind turbines. Renew Energy 2016; 86, 49-58.

[16] Prowell I, Veletzos M, Elgamal A, Restrepo J. Experimental and numerical seismic response of a 65 kW wind turbine. J Earthq Eng 2009; 13(8): 1172-1190.

[17] Prowell I. An experimental and numerical study of wind turbine seismic behavior. PhD dissertation, University of California, San Diego; 2011.

[18] Prowell I, Elgamal A, Uang C, Luco JE, Romanowitz H, Duggan E. Shake table testing and numerical simulation of a utility-scale wind turbine including operational effects. Wind Energy 2014; 17(7): 997-1016.

[19] Zhao X, Maisser P. Seismic response analysis of wind turbine towers including soil-structure interaction. Proc. Inst. Mech. Eng. Part H-J. Eng. Med 2006; 220(1): 53-61.

[20] Zhao X, Maisser P, Wu J. A new multibody modelling methodology for wind turbine structures using a cardanic joint beam element. Renew Energy (2007); 32: 532-546.

[21] Jonkman JM, Buhl ML. FAST user's guide. Golden: National Renewable Energy Laboratory; 2005.

[22] Asareh MA, Prowell I. Seismic loading for FAST. Subcontract Report No. NREL/SR-5000-53872. Rolla: Missouri University of Science and Technology; 2011.

[23] Asareh MA, Prowell I. NWTC design code FAST-Seismic. https://nwtc.nrel.gov/Seismic (Accessed 9 Nov. 2015); 2012.

[24] Haenler M, Ritschel U, Warnke I. Systematic modelling of wind turbine dynamics and earthquake loads on wind turbines. In: Proceedings of the European Wind Energy Conference & Exhibition (EWEC), Athens, Greece, 27 February - 2 March 2006.

[25] Witcher D. Seismic analysis of wind turbines in the time domain. Wind Energy 2005; 8(1): 81-91.

[26] Bossanyi E. Bladed for Windows user manual. Bristol: Garrad Hassan and Partners; 2000.

[27] Valamanesh V, Myers AT. Aerodynamic damping and seismic response of horizontal axis wind turbine towers. J Struct Eng 2014; 140(11), 04014090.

[28] Asareh MA, Volz JS. Evaluation of aerodynamic and seismic coupling for wind turbines using finite element approach. In: Proceedings of ASME 2013 International Mechanical Engineering Congress and Exposition, Vol. 4B - Dynamics, Vibration and Control, San Diego, California, 15-21 November 2013.

[29] International Electrotechnical Commission (IEC). Wind turbine generator systems. Part 1: Safety requirements. IEC 61400-1 (Ed. 3). Geneva: International Electrotechnical Commission; 2005.

[30] American Society of Civil Engineers/American Wind Energy Association (ASCE/AWEA). Recommended practice for compliance of large land-based wind turbine support structures. ASCE/AWEA RP2011. Reston/Washington: American Society of Civil Engineers/American Wind Energy Association; 2011.

[31] Asareh M-A, Prowell I. A simplified approach for implicitly considering aerodynamics in the seismic response of utility scale wind turbines. In: Proceedings of 53rd AIAA/ASME/ASCE/AHS/ASC Structures, Structural Dynamics and Materials Conference, Honolulu, Hawaii, 23-26 April 2012.

[32] American Petroleum Institute (API). Recommended practice for planning, designing and constructing fixed offshore platforms – Working stress design. API RP 2A-WSD (21st Ed.). Washington: American Petroleum Institute; 2000.

[33] Zaaijer MB. Foundation modelling to assess dynamic behaviour of offshore wind turbines. Appl Ocean Res 2006; 28: 45-57.

[34] Jonkman J, Musial W. Offshore Code Comparison Collaboration (OC3) for IEA Task 23 Offshore Wind Technology and Deployment. Technical Report No. NREL/TP-5000-48191. Golden: National Renewable Energy Laboratory; 2010.

[35] AlHamaydeh M, Hussain S. Optimized frequency-based foundation design for wind turbine towers utilizing soil–structure interaction. J. Frankl. Inst.-Eng. Appl. Math. 2011; 348(7): 1470-1487.

[36] Rendon EA, Manuel L. Long-term loads for a monopile-supported offshore wind turbine. Wind Energy 2014; 17(2): 209-223.

[37] Carswell W, Arwade SR, DeGroot DJ, Lackner MA. Soil-structure reliability of offshore wind turbine monopile foundations. Wind Energy 2015; 18(3): 483-498.

[38] Kavvadas M, Gazetas G. Kinematic seismic response and bending of free-head piles in layered soil. Géotechnique 1993; 43(2): 207-222.

[39] Makris N, Gazetas G, Delis E. Dynamic soil-pile-foundation-structure interaction: records and predictions. Géotechnique 1996; 46(1): 33-50.

[40] Bisoi S, Haldar S. Dynamic analysis of offshore wind turbine in clay considering soil-monopile-tower interaction. Soil Dyn Earthq Eng 2014; 63: 19-35.

[41] Bisoi S, Haldar S. Design of monopile supported offshore wind turbine in clay considering dynamic soil-structure-interaction. Soil Dyn Earthq Eng 2015; 73: 103-117.

[42] Boulanger RW, Curras CJ, Kutter BL, Wilson DW, Abghari A. Seismic soil-pile-structure interaction experiments and analyses. J Geotech Geoenviron Eng 1999, 125(9): 750-759.

[43] Assareh MA, Asgarian B. Nonlinear behavior of single piles in jacket type offshore platforms using incremental dynamic analysis. Am J Appl Sci 2008; 5(12): 1793-1803.

[44] Makris N, Gazetas G. Displacement phase differences in a harmonically oscillating pile. Géotechnique 1993; 43(1): 135-150.

[45] Mostafa YE, El Naggar MH. Response of fixed offshore platforms to wave and current loading including soil–structure interaction. Soil Dyn Earthq Eng. 2004; 24: 357-368.

[46] El Naggar MH, Novak M. Nonlinear analysis for dynamic lateral pile response. Soil Dyn Earthq Eng 1996; 15: 233-244.

[47] Gazetas G. Formulas and charts for impedances of surface and embedded foundations. J Geotech Eng 1991; 117(9): 1363-1381.

[48] Manwell JF, McGowan JG, Rogers AL. Wind energy explained: Theory, design and application. Chichester: John Wiley & Sons; 2010.

[49] Pacific Earthquake Engineering Research Center (PEER). Peer ground motion database. University of California, Berkeley, 2013 (http://ngawest2.berkeley.edu/).

[50] Raychowdhury P. Seismic response of low-rise steel moment-resisting frame (SMRF) buildings incorporating nonlinear soil–structure interaction (SSI). Eng Struct 2011; 33(3): 958-967.

[51] Raychowdhury P, Hutchinson TC. Performance evaluation of a nonlinear Winkler-based shallow foundation model using centrifuge test results. Earthq Eng Struct Dyn 2009; 38: 679-698.

[52] Allotey N, El Naggar MH. An investigation into the Winkler modeling of the cyclic response of rigid footings. Soil Dyn Earthq Eng 2008; 28: 44-57.

[53] Alati N, Failla G, Arena A. Seismic analysis of offshore wind turbines on bottom-fixed support structures. Phil. Trans. R. Soc. A 2015; 373(2035): 20140086.

[54] Failla G, Arena F. New perspectives in offshore wind energy. Phil. Trans. R. Soc. A 2015; 373(2035): 20140228.

FIGURE CAPTIONS

Fig. 1. 5 MW three-bladed HAWT with a steel column, resting on a concrete pile-supported square footing.

Fig. 2. Geometry and sign conventions for stress resultants at the tower base (length in m, diameter and thickness in mm).

Fig. 3. Lateral and vertical springs along piles (length in m).

Fig. 4. First and second FA support structure modes for (a) fixed foundation, (b) flexible foundation.

Fig. 5. 5% damped SRSS pseudo spectral acceleration for earthquake records in Table 3.

Fig. 6. Fixed foundation: Errors (2)-(3) for various potential aerodynamic damping values, under various earthquakes in Table 3.

Fig. 7. Fixed foundation: Errors (2) for 4% aerodynamic damping, under all earthquakes in Table 3.

Fig. 8. Fixed foundation: SRSS bending moment and shear force at the tower base under Northridge earthquake and a wind sample for V=11.4 m/s at the hub; (a) earthquake response with 4% aerodynamic damping (AD), (b) operational wind response, (c) comparison between fully-coupled simulation and combination of uncoupled analyses, with a 4% aerodynamic damping in the earthquake response.

Fig. 9. Fixed foundation: mean bending-moment demands along the tower, for all earthquakes in Table 3.

Fig. 10. Fixed foundation: mean shear-force demands along the tower, for all earthquakes in Table 3.

Fig. 11. Flexible foundation with 5% structural damping ratio in support structure modes: Errors (2)-(3) for various potential aerodynamic damping values, under various earthquakes in Table 3.

Fig. 12. Flexible foundation with 5% structural damping ratio in support structure modes: Errors (2) for 4% aerodynamic damping, under all earthquakes in Table 3.

Fig. 13. Flexible foundation with 5% structural damping ratio in support structure modes: mean bending-moment demands along the tower, for all earthquakes in Table 3.

Fig. 14. Flexible foundation with 5% structural damping ratio in support structure modes: mean shear-force demands along the tower, for all earthquakes in Table 3.

Fig. 15. Flexible foundation with 5% structural damping ratio in support structure modes: maxima *x*-deflections along pile #1, for some wind samples in Table 3.

Fig. 16. Flexible foundation with 20% structural damping ratio in support structure modes: Errors (2)-(3) for various potential aerodynamic damping values, under various earthquakes in Table 3.

Fig. 17. Flexible foundation with 20% structural damping ratio in support structure modes: Errors (2) for 4% aerodynamic damping, under all earthquakes in Table 3.

Fig. 18. Flexible foundation with 20% structural damping ratio in support structure modes: mean bending-moment demands along the tower, for all earthquakes in Table 3.

Fig. 19. Flexible foundation with 20% structural damping ratio in support structure modes: mean shear-force demands along the tower, for all earthquakes in Table 3.

Fig. 20. Flexible foundation with 20% structural damping ratio in support structure modes: maxima *x*-deflections along pile #1, for some wind samples in Table 3.

TABLE CAPTIONS

Table 1. Wind turbine parameters, material and soil properties.

Table 2. Natural frequencies for fixed and flexible foundation models.

Table 3. Earthquake records and wind velocities at the hub.